

*Thesis*  
*On*  
**ANALYSIS AND MODELING OF MRR, TWR AND SR PARAMETERS IN  
DRILLING OF GLASS FIBER REINFORCED COMPONENTS USING  
FUZZY LOGIC**

*Submitted in the fulfillment of the requirement for  
the award of degree of*  
**MASTER OF ENGINEERING**  
**IN**  
**PRODUCTION AND INDUSTRIAL ENGINEERING**

*Submitted By*  
**PAWAN KUMAR**  
**Roll No. 801082024**

Under the Guidance of  
**Dr. V.K. SINGLA**  
Associate Professor  
Department of Mechanical Engineering  
Thapar University, Patiala - 147004



**DEPARTMENT OF MECHANICAL ENGINEERING**  
**THAPAR UNIVERSITY**  
**PATIALA-147004, INDIA**  
**JULY, 2012**

## **ACKNOWLEDGEMENT**

*Words are often less to reveal one's deep regards. With an understanding that work like this can never be the outcome of a single person, I take this opportunity to express my profound sense of gratitude and respect to all those who directly or indirectly helped me through the duration of this work.*

*I take the opportunity to express my heartfelt adulation and gratitude to my supervisor, **Dr. V.K. SINGLA** for their unreserved guidance, constructive suggestions, thought provoking discussions and unabashed inspiration in the nurturing work. It has been a benediction for me to spend many opportune moments under the guidance of the perfectionist at the acme of professionalism. The present work is testimony to their activity, inspiration and ardent personal interest, taken by them during the course of this work in its present form. I am grateful to **Dr. Ajay Batish**, Prof. & Head, MED and **Dr. S.K Mohapatra**, Dean of Academic Affairs for providing the facilities for the completion of the work.*

*I take pride of myself being son of ideal parents for their everlasting desire, sacrifice, affectionate blessings, and help, without which it would not have been possible for me to complete my studies.*

*I would like to thank to all the members and employees of Mechanical Engineering Department, Thapar University Patiala for their everlasting support. Above all, I express my indebtedness to the "ALMIGHTY" for all his blessing and kindness.*

**Pawan Kumar**  
**Registration No.: 801082024**

## DECLARATION

I hereby declare that the thesis entitled "ANALYSIS AND MODELING OF MRR, TWR AND SR PARAMETERS IN DRILLING OF GLASS FIBER REINFORCED COMPONENTS USING FUZZY LOGIC" is an authentic record of my study carried out as requirement for the award of degree of **Master of Engineering (Production and Industrial Engineering)** at **Thapar University, Patiala** under the guidance of **Dr.V.K.SINGLA**, Associate Professor, Department of Mechanical Engineering, Thapar University, Patiala. The matter embodied in this report has not been submitted in part or full to any other University or Institute for the award of any other degree.



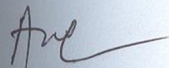
**(Pawan Kumar)**  
**Reg. No. 801082024**

This is to certify that above declaration made by the student concerned is correct to the best of my knowledge and belief.



**(Dr. V.K. SINGLA)**  
Associate Professor  
Department of Mechanical Engineering  
Thapar University, Patiala - 147004

*Countersigned by*



**Dr. AJAY BATISH**  
Professor and Head  
Department of Mechanical Engineering  
Thapar University, Patiala -147004



**Dr. S.K. MOHAPATRA**  
Dean of Academic Affairs  
Thapar University, Patiala -147004

## **Abstract**

---

The GFRP (glass fibre reinforced composite materials) are find up numerous application in many engineering and domestic fields due to their excellent mechanical properties and corrosion resistance. Among the machining process used drilling is one of the most important process and is mainly used for joining of composite structures. Maintain of proper surface roughness in drilling hole is very important and is to be controlled. In the present work material removal rate (MRR), tool wear rate (TWR), and surface roughness (SR) parameters have been studied for analysis and have been modelled. A fuzzy rule based model will be developed to predict the response parameter in drilling of glass fibre reinforced composite.

## ABBREVIATIONS

---

AI	-	artificial intelligence
I/P	-	input
O/P	-	output
W/P	-	work piece
OA	-	orthogonal array
DOF	-	degree of freedom
SR	-	surface roughness
MRR	-	material removal rate
TWR	-	tool wear rate
CI	-	confidence interval
FL	-	fuzzy logic
MF	-	membership function
ANOVA	-	analysis of variance
DOE	-	design of experiment

# CONTENTS

---

<b>TITLE</b>	<b>PAGE NO.</b>
<b>ACKNOWLEDGEMENTS</b>	i
<b>DECLARATION</b>	ii
<b>ABBREVIATIONS</b>	iii
<b>LIST OF FIGURES</b>	viii
<b>LIST OF TABLES</b>	x
<b>CHAPTER 1 INTRODUCTION</b>	1-12
1.1 Introduction	1
1.2 Drilling Operation	1
1.2.1 General-Purpose Drilling Machines	2
1.2.2 Radial Drilling Machines	2
1.2.3 Drilling allied Operations	3
1.3 Composite Material	4
1.3.1 Fibers	5
1.3.2 Matrices	5
1.4 Advantages and Disadvantages of Composite Materials	6
1.5 Applications	6
1.6 Surface Roughness	6
1.6.1 Average Surface Roughness, $R_a$	6
1.6.2 Root Mean Square Roughness, $R_q$	7
1.6.3 Surface Profile Measurement Lengths	7

1.7 Tool Wear	8
1.7.1 Tool Wear Regions	8
1.8 Fuzzy Logic	9
1.8.1 Fuzzy Sets	10
1.8.2 Operations on Fuzzy Sets	10
1.8.3 Fuzzy Complements	11
1.8.4 Fuzzy Intersection	11
1.8.5 Fuzzy Unions	12
1.8.6 Membership Functions	12
<b>CHAPTER 2 LITERATURE REVIEW</b>	<b>13-18</b>
2.1 Cutting Force	13
2.2 Tool Wear	14
2.3 Optimization of Process Parameter	16
2.4 Surface Roughness	17
2.5 Delamination	18
<b>CHAPTER 3 EXPERIMENTATION</b>	<b>19-29</b>
3.1 Introduction	19
3.2 Drilling Machine	19
3.3 Work piece	20
3.4 Tool	20
3.4 DOE	21
3.5 Orthogonal Array	22
3.6 Drilling Process	23
3.7 Analysis of Result	28

<b>CHAPTER 4 RESULT AND ANALYSIS</b>	30-47
4.1 Introduction	30
4.2 Results for MRR	30
4.2.1 ANOVA for MRR	31
4.2.2 ANOVA for S/N Ratio of MRR	34
4.2.3 Optimal Design for MRR	36
4.2.4 Estimated Result at Optimum Condition	36
4.2.5 Confidence Interval of Result at Optimum Condition	36
4.3 Results for Surface Roughness	37
4.3.1 ANOVA for SR	38
4.3.2 ANOVA for S/N of SR	40
4.3.3 Optimal Design for SR	42
4.3.4 Estimated Result at Optimum Condition	43
4.3.5 Confidence Interval around the Estimated Mean	43
4.4 Tool Wear	43
<b>CHAPTER 5 FUZZY MODELING AND ANALYSIS</b>	48-60
5.1 Introduction	48
5.2 Fuzzification	48
5.3 Membership Functions	48
5.3.1 Triangular MF	49
5.3.2 Trapezoidal MF	50
5.4 Rule Evaluation	52
5.5 Defuzzification	54
5.6 Analysis of Fuzzy Results	55
5.6.1 Correlation Graphs	56

5.6.2 Response Surface Plots	58
<b>CHAPTER 6 RESULTS AND DISCUSSION</b>	61-62
6.1 Results and Discussion	61
6.1.1 MRR	61
6.1.2 SR	61
6.1.3 TWR	61
6.1.4 Fuzzy Modeling	62
<b>REFERENCES</b>	63-65
<b>APPENDIX</b>	66-69

## LIST OF FIGURES

---

<b>FIGURE CAPTION</b>	<b>PAGE NO.</b>
Figure 1.1 Drilling operation	1
Figure 1.2 Radial drilling machine	3
Figure 1.3 Drilling and drilling allied operations	3
Figure 1.4 Reinforcement Options	4
Figure 1.5 Surface roughness profile	7
Figure 1.6 Profile measurement lengths	7
Figure 1.7 Types wear on cutting tools	8
Figure 1.8 Types of tool wear	9
Figure 1.9 Representation of rigid (left) and flexible (right) statement	12
Figure 3.1 GFRP plate	20
Figure 3.2 Drill bits	21
Figure 3.3 Schematic of drilling process	23
Figure 3.4 Force plot for 1 trial run	27
Figure 3.5 Model of drilling system	29
Figure 4.1 Main effects plot for MRR	33
Figure 4.2 Interaction plot for MRR	33
Figure 4.3 Main effects plot of MRR for S/N ratio	35
Figure 4.4 Interaction plot of MRR for S/N ratio	35
Figure 4.5 Main effects plot for SR	39
Figure 4.6 Interaction plot for SR	40
Figure 4.7 Main effects plot of SR for S/N ratio	41

## LIST OF FIGURES

---

FIGURE CAPTION	PAGE NO.
Figure 4.8 Interaction plot of TWR for S/N ratio	42
Figure 4.9 Torque Vs hole number	46
Figure 4.10 Tool Wear after different number of hole	46
Figure 4.11 Tool wear Vs Hole number	47
Figure 5.1 Triangular MF for (a) feed, (b) speed, (c) drill diameter, (d) point angle, (e) SR, (f) MRR	49-50
Figure 5.2 Trapezoidal MF for (a) feed, (b) speed, (c) drill diameter, (d) point angle, (e) SR, (f) MRR	51-52
Figure 5.3 Defuzzifier for triangular MF	54
Figure 5.4 Predicted Vs Experimental MRR	55
Figure 5.5 Predicted Vs Experimental SR	55
Figure 5.6 Correlation graph for triangular MF for SR	56
Figure 5.7 Correlation graph for trapezoidal MF for SR	56
Figure 5.8 Correlation graph for triangular MF for MRR	57
Figure 5.9 Correlation graph for trapezoidal MF for MRR	57
Figure 5.10 Response surface between point angle and speed for SR	58
Figure 5.11 Response surface between point angle and drill diameter for SR	59
Figure 5.12 Response surface between point angle and speed for MRR	59
Figure 5.13 Response surface between point angle and drill diameter for MRR	60

## LIST OF TABLES

---

TABLE CAPTION	PAGE NO.
Table 1.1 Properties of typical high strength fibers	5
Table 3.1 Technical specification of drilling machining	19
Table 3.2 Properties of W/P material	20
Table 3.3 Factors and their levels	21
Table 3.4 Calculation of DOF	22
Table 3.5 L <sub>18</sub> OA	22-23
Table 3.6 Drilling force table foe 1 trial run	24-26
Table 3.7 Drilling force table for all trial run	27-28
Table 3.8 Various response characteristics	28
Table 4.1 Trial results for MRR	30-31
Table 4.2 ANOVA for means of MRR	32
Table 4.3 Response Table for Means of MRR	32
Table 4.4: ANOVA for S/N of MRR	34
Table 4.5 Response table for S/N ratio of MRR	34
Table 4.6 Significant factors and interactions	36
Table 4.7 Trial results for SR	37-38
Table 4.8 ANOVA For means of SR	38
Table 4.9 Response Table for Means of SR	39
Table 4.10 ANOVA for S/N of SR	40-41
Table 4.11 Response table for S/N ratio of SR	41

## LIST OF TABLES

---

<b>TABLE CAPTION</b>	<b>PAGE NO.</b>
Table 4.12 Significant factors and interactions	42-43
Table 4.13 Force table for tool wear	44-45
Table 4.14 Wear variation with number of hole	47
Table 5.1 Fuzzification of variables	48

# CHAPTER 1

## INTRODUCTION

---

### 1.1 INTRODUCTION

The GFRP (glass fibre reinforced composite materials) are found in numerous applications in many engineering and domestic fields due to their excellent mechanical properties and corrosion resistance. Among the machining processes used, drilling is one of the most important processes and is mainly used for joining of composite structures. Maintaining proper surface roughness in a drilled hole is very important and must be controlled. Since the surface properties do not remain the same before and after drilling, a poor drilled hole surface may cause the formation and progression of cracks at a rapid rate, so it must be controlled. In the present work, material removal rate (MRR), tool wear rate (TWR), and surface roughness (SR) parameters have been studied for analysis and have been modelled. A fuzzy rule-based model has been developed to predict the response parameter in drilling of glass fibre reinforced composite.

### 1.2 DRILLING OPERATION

Drilling is a process used extensively by which through or blind holes are prepared in a workpiece (W/P). This process involves feeding a rotating cutting tool (drill) along its axis of rotation into a stationary W/P (Figure 1.1). The axial feed rate  $f$  is usually very small as compared to the peripheral speed  $v$ . Drilling is considered a roughing operation and, therefore, the accuracy and surface finish in drilling are generally not of much concern. If high accuracy and good finish are required, drilling is followed by some other operation such as reaming or boring. Drilling in some cases is considered a primary operation and in some cases it is considered a final operation.

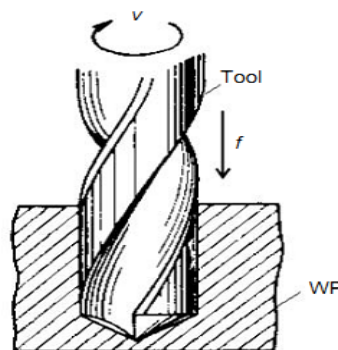


Figure 1.1 Drilling operation [1]

### **1.2.1 GENERAL-PURPOSE DRILLING MACHINES**

The general-purpose drilling machines can be classified as

1. Bench-type sensitive drill presses
2. Upright drill presses
3. Radial drills
4. Multi spindle drilling machines
5. Horizontal drilling machines for drilling deep holes

### **1.2.2 RADIAL DRILLING MACHINES**

These machines are especially designed for drilling, counter boring, countersinking, reaming, and tapping holes in heavy and bulky W/Ps that are inconvenient or impossible to machine on the upright drilling machines. They are suitable for multi tool machining in individual and batch production. Radial drilling machines (Figure 1.2) differ from upright drill presses in that the spindle axis is made to coincide with the axis of the hole being machined by moving the spindle in a system of polar coordinate to the hole, while the work is stationary. This is achieved by

1. Swinging the radial arm (4) about the rigid column (2)
2. Raising or lowering the radial arm on the column by the arm-elevating and –clamping mechanism (3) to accommodate the W/P height
3. Moving the spindle head (5) along the guide ways of the radial arm (4)

Accordingly, the tool is located at any required point on the stationary WP, which is set either on detachable table (6) or directly on base (1). After the maneuvering tasks performed by the radial arm and spindle head, they are held in position using power-operated clamping devices.

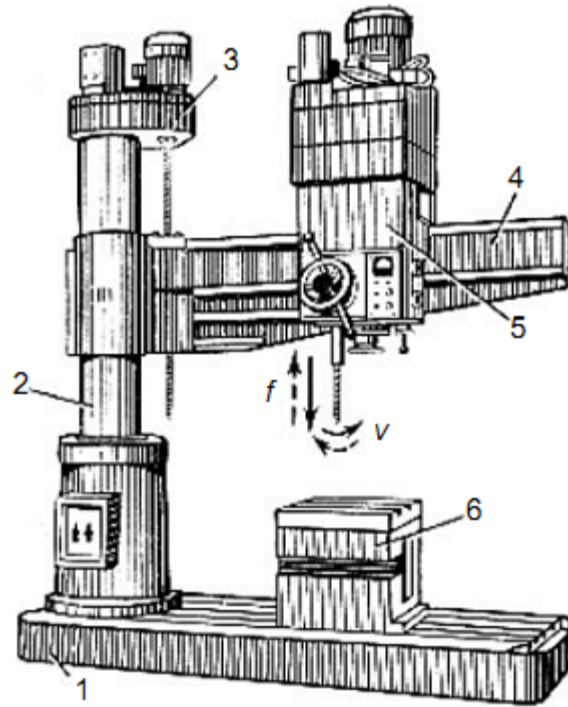


Figure 1.2 Radial drilling machine [1]

### 1.2.3 DRILLING ALLIED OPERATIONS

Drilling allied or alternative operations such as core drilling, center drilling, counter boring, countersinking, spot facing, reaming, tapping, and other operations can also be performed on drilling machines as shown in Figure 1.3.

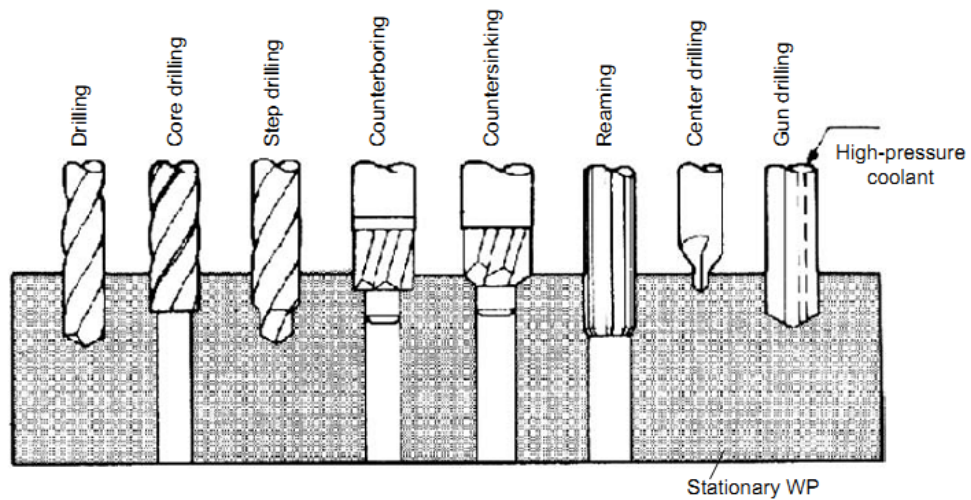


Figure 1.3 Drilling and drilling allied operations [1]

### 1.3 COMPOSITE MATERIAL

A composite material can be defined as a combination of two or more materials that results in better properties than when the individual components are used alone. As opposed to metal alloys, each material retains its separate chemical, physical and mechanical properties. The two constituents are normally a fiber (reinforcement) and a matrix. Typical fibers include glass, aramid and carbon, which may be continuous or discontinuous. Matrices can be polymers, metals or ceramics. So based on matrix composites can be classified as,

- polymeric composites
- metallic composites
- ceramic composites

Examples of continuous reinforcements include unidirectional, woven cloth and helical winding, while discontinuous reinforcements include chopped fibers and random mat (Fig. 1.4).

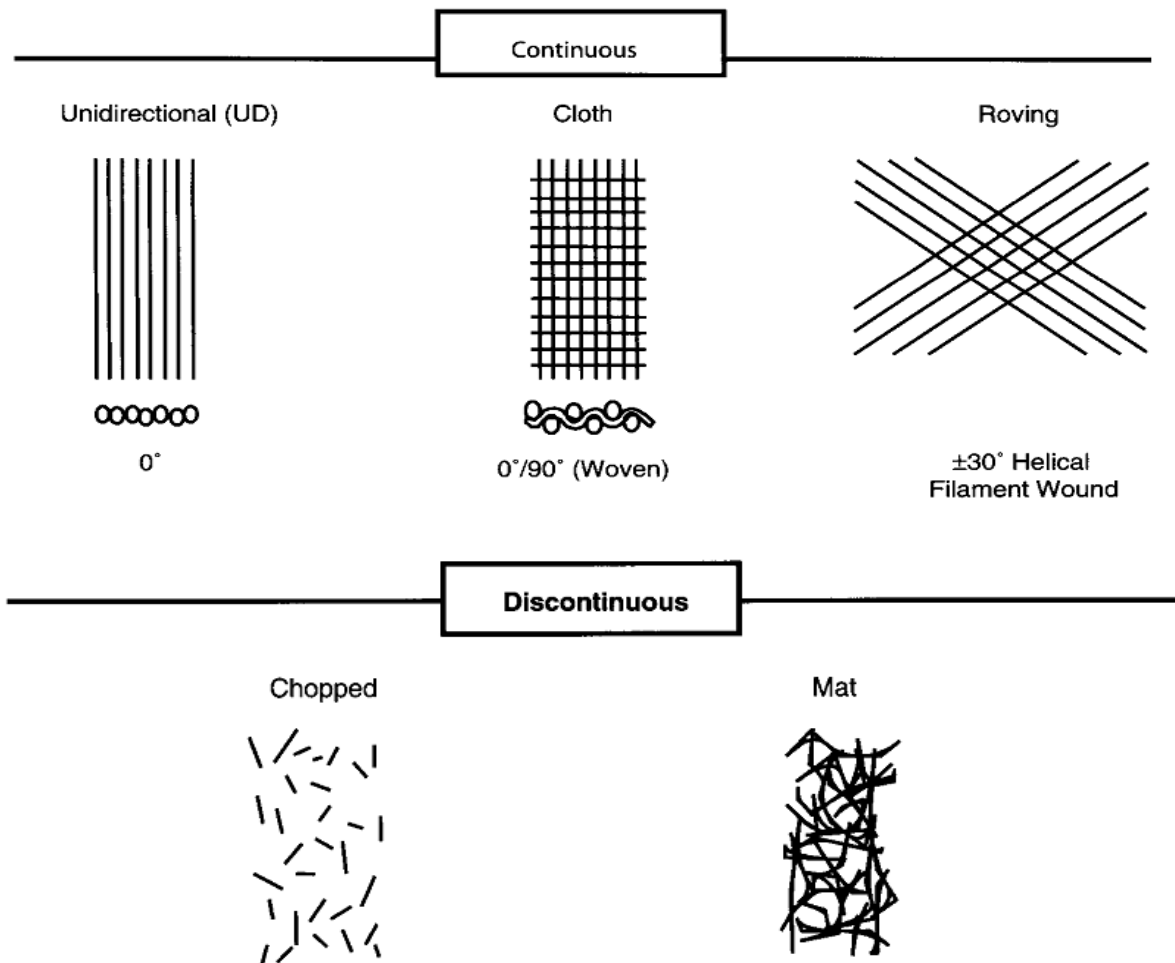


Figure 1.4 Reinforcement Options [2]

### 1.3.1 FIBERS

The primary role of the fibers is to provide strength and stiffness. However, as a class, high-strength fibers are brittle; possess linear stress-strain. Glass fibers are the most widely used reinforcement due to their good balance of mechanical properties and low cost. Properties of typical high strength fibers is tabulated below (table 1.1).

**Table 1.1 Properties of typical high strength fibers**

<i>Fiber</i>	<i>Density lb/in<sup>3</sup></i>	<i>Tensile Strength (ksi)</i>	<i>Elastic Modulus (msi)</i>	<i>Strain to Failure (%)</i>	<i>Diameter (Mils)</i>	<i>Thermal Expansion Coefficient 10<sup>-6</sup> in/in/ F</i>
E-glass	0.090	500	11.0	4.8	0.36	2.8
S-glass	0.092	650	12.6	5.6	0.36	1.3
Quartz	0.079	490	10.0	5.0	0.35	1.0
Aramid (Kelvar 49)	0.052	550	19.0	2.8	0.47	-1.1
Spectra 1000	0.035	450	25.0	0.7	1.00	-1.0
Carbon (AS4)	0.065	530	33.0	1.5	0.32	-0.2
Carbon (IM-7)	0.064	730	41.0	1.8	0.20	-0.2
Graphite (P-100)	0.078	350	107	0.3	0.43	-0.3
Boron	0.093	520	58.0	0.9	4.00	2.5

### 1.3.2 MATRICES

The matrix holds the fibers in their proper position, protects the fibers from abrasion, transfers loads between fibers, and provides inter laminar shear strength. A properly chosen matrix also provides resistance to heat, chemicals and moisture; it has a high strain-to-failure; and it cures at as low a temperature as possible and yet has a long pot or out-time life and is not toxic. The most prevalent thermoset resins used for composite matrices are polyesters, vinyl esters, epoxies, bismaleimides, polyimides and phenolics. Matrices for polymeric composites can be either thermosets or thermoplastics. Thermoset resins usually consist of a resin (e.g., epoxy) and a compatible curing agent. When the two are initially mixed they form a low-viscosity liquid that cures as a result of either internally generated (exothermic) or externally applied heat. The curing reaction forms a series of cross-links between the molecular chains so that one large molecular network is formed, resulting in an intractable solid that cannot be reprocessed on reheating. On the other hand, thermoplastics start as fully reacted high-viscosity materials that do not cross-link on heating. On heating to a high enough temperature, they either soften or melt, so they can be reprocessed a number of times.

## 1.4 ADVANTAGES AND DISADVANTAGES OF COMPOSITE MATERIALS

Advantages of composites

- lighter weight
- the ability to tailor the lay-up for optimum strength and stiffness
- improved fatigue life
- corrosion resistance and
- with good design practice, reduced assembly costs due to fewer detail parts and fasteners

Disadvantages of composites

- their raw material costs are high, and they usually incur high fabrication and assembly costs
- these are adversely affected by both temperature and moisture
- they are weak in the out-of-plane direction where the matrix carries the primary load and should not be used where load paths are complex (e.g., lugs and fittings)
- composite are susceptible to impact damage and delaminations or ply separations can occur and
- these are more difficult to repair than metallic structures

## 1.5 APPLICATIONS

The use of composite materials is extensive and expanding. Applications include aerospace, automotive, marine, sporting goods and infrastructure.

## 1.6 SURFACE ROUGHNESS

Surface roughness is a very important characteristics as it affects the functional characteristics of products such as resisting fatigue, friction, wearing, light reflection, heat transmission, and lubrication [3]. There are many SR measure characteristics such as Rz, Rq, Rt but average surface roughness Ra is the most common index for determining surface quality.

### 1.6.1 AVERAGE SURFACE ROUGHNESS, $R_a$

Roughness average Ra is the arithmetic average of the absolute values of the roughness profile ordinates as shown in figure.1.5.

$$R_a = \frac{1}{l} \int_0^l |Z(x)| dx$$

(Eq. 1.1)

### 1.6.2 ROOT MEAN SQUARE ROUGHNESS, $R_q$

Root mean square (RMS) roughness  $R_q$  is the root mean square average of the roughness profile ordinates. It is calculated using following formula,

$$R_q = \sqrt{\frac{1}{l} \int_0^l Z^2(x) dx}$$

(Eq. 1.2)

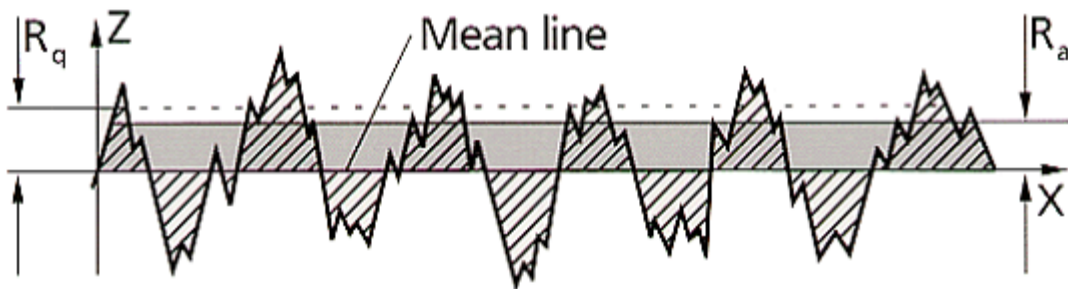


**Figure 1.5 Surface roughness profile [4]**

$R_a$  is also called AA and CLA.

### 1.6.3 SURFACE PROFILE MEASUREMENT LENGTHS

The various profile measurement length are defined and shown below.

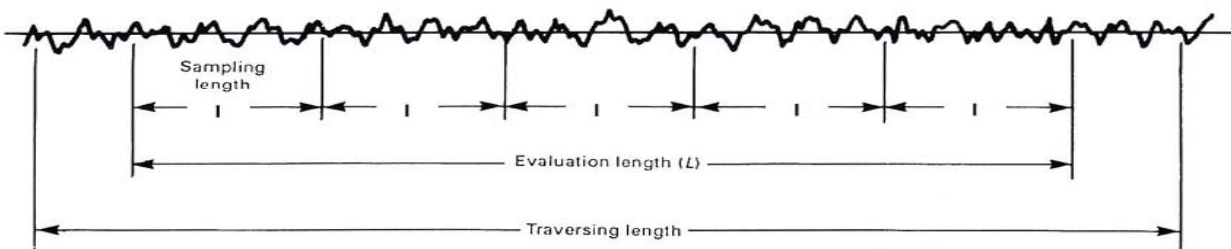


**Figure 1.6 Profile measurement lengths [4]**

Traversing length ( $l_t$ ) is the overall length traveled by the stylus when acquiring the traced profile. It is the sum of pre-travel, evaluation length ( $l_n$ ) and post-travel. Sampling length ( $l_r$ ) is the reference for roughness evaluation. Its length is equal to the cutoff wavelength ( $\lambda_c$ ). The sampling lengths  $l_p$  and  $l_w$ , respectively, are the reference lengths for the P-profile and the W-profile evaluation. Evaluation length  $l_n$  is that part of the traversing length  $l_t$  over which the

values of surface parameters are determined. The standard roughness evaluation length comprises five consecutive sampling lengths.

## 1.7 TOOL WEAR

Tool wear leads to tool failure. The failure of cutting tool occurs as premature tool failure (i.e., tool breakage) and progressive tool wear. Figure 1.7 shows some types of failures and wear on cutting tools. Generally, wear of cutting tools depends on tool material and geometry, work-piece materials, cutting parameters (cutting speed, feed rate and depth of cut), cutting fluids and machine-tool characteristics.

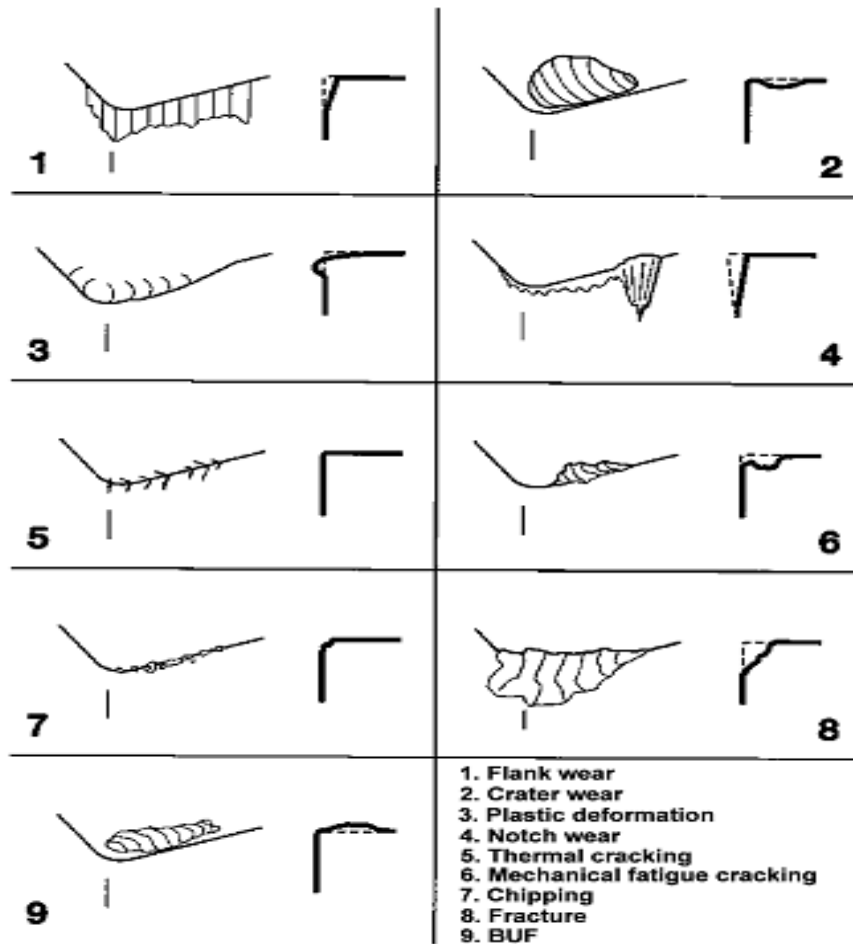


Figure 1.7 Types wear on cutting tools [5]

### 1.7.1 TOOL WEAR REGIONS

Normally, tool wear is a gradual process. There are two basic zones of wear in cutting tools: flank wear and crater wear. Flank and crater wear are the most important measured forms of tool wear. Flank wear is most commonly used for wear monitoring. According to the standard ISO

3685:1993 for wear measurements, the major cutting edge is considered to be divided in to four regions, as shown in Figure 2.11:

- Region C is the curved part of the cutting edge at the tool corner;
- Region B is the remaining straight part of the cutting edge in zone C;
- Region A is the quarter of the worn cutting edge length  $b$  farthest away from the tool corner;
- Region N extends beyond the area of mutual contact between the tool work piece for approximately 1–2 mm along the major cutting edge. The wear is of notch type.

The width of the flank wear land,  $VB_B$ , is measured within zone B in the cutting edge plane  $P_s$  perpendicular to the major cutting edge. The width of the flank wear land is measured from the position of the original major cutting edge. The crater depth,  $KT$ , is measured as the maximum distance between the crater bottom and the original face in region B.

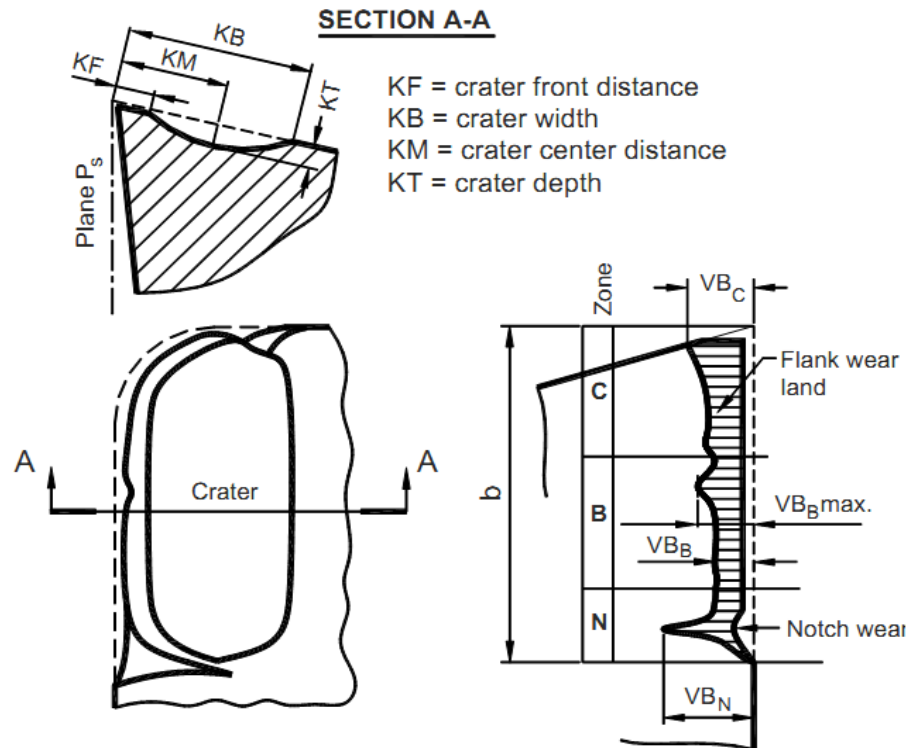


**Figure 1.8 Types of tool wear [8]**

## 1.8 FUZZY LOGIC

Fuzzy logic poses the ability to mimic the human mind to effectively employ modes of reasoning that are approximate rather than exact. Precision and certainty carry a cost. But in our life many times we deal with uncertainty, so the concept of FL originated. Fuzzy logic resembles human decision making with its ability to work from approximate data and find precise solutions. Fuzzy

logic is a continuous form of logic. It allows modelling complex systems using a higher level of abstraction originating from our knowledge and experience.

### 1.8.1 FUZZY SETS

Zadeh introduced the term fuzzy logic in his seminal work “Fuzzy sets,” which described the mathematics of fuzzy set theory (1965). Plato laid the foundation for what would become fuzzy logic, indicating that there was a third region beyond True and False. A fuzzy set is an extension of a crisp set. Crisp sets allow only full membership or no membership at all, whereas fuzzy sets allow partial membership. In a crisp set, membership or nonmembership of element  $x$  in set  $A$  is described by a characteristic function, where and . Fuzzy set theory extends this concept by defining partial membership. A fuzzy set  $A$  on a universe of discourse  $U$  is characterized by a membership function that takes values in the interval .

The characteristic function of a crisp set assigns a value of either 1 or 0 to each individual in the universal set, thereby discriminating between members and non members of the crisp set under consideration. This function can be generalized such that the values assigned to the elements of the universal set fall within a specified range and indicate the membership grade of these elements in the set in question. Larger values denote higher degrees of set membership. Such a function is called a membership function, and the set defined by it a fuzzy set. The most commonly used range of values of membership functions is the unit interval  $[0, 1]$ . In this case, each membership function maps elements of a given universal set  $X$ , which is always a crisp set, into real numbers in  $[0, 1]$ .

Two distinct notations are most commonly employed in the literature to denote membership functions. In one of them, the membership function of a fuzzy set  $A$  is denoted by  $\mu_A$ ; that is,  $\mu_A: X \rightarrow [0, 1]$ .

In the other one, the function is denoted by  $A$  and has of course, the same form:

$$A : X \rightarrow [0, 1].$$

According to the first notation, the symbol (label, identifier, name) of the fuzzy set ( $A$ ) is distinguished from the symbol of its membership function ( $\mu_A$ ). According to the second notation, this distinction is not made, but no ambiguity results from this double use of the same symbol. Each fuzzy set is completely and uniquely defined by one particular membership function; consequently, symbols of membership functions may also be used as labels of the associated fuzzy sets.

### 1.8.2 OPERATIONS ON FUZZY SETS

The standard fuzzy operations are generalizations of the corresponding classical set operations. The standard fuzzy operations perform precisely as the corresponding operations for crisp sets. Following are the special operations of fuzzy complement, intersection, and Union

$$\bar{A}(x) = 1 - A(x),$$

$$(A \cap B)(x) = \min[A(x), B(x)],$$

$$(A \cup B)(x) = \max[A(x), B(x)]$$

$$x \in X.$$

These operations are called the standard fuzzy operations. For each of the three operations, there exists a broad class of functions whose members qualify as fuzzy generalizations of the classical operations as well. Functions that qualify as fuzzy intersections and fuzzy unions are usually referred as t-norms and t-conorms, respectively. The standard fuzzy intersection (min operator) produces for any given fuzzy sets the largest fuzzy set from among those produced by all possible fuzzy intersections (r -norms). The standard fuzzy union (max operator) produces, on the contrary, the smallest fuzzy. Set among the fuzzy sets produced by all possible fuzzy unions (t -conorms). That is, the standard fuzzy operations occupy specific positions in the whole spectrum of fuzzy operations: the standard fuzzy intersection is the weakest fuzzy intersection, while the standard fuzzy union is the strongest fuzzy union.

### 1.8.3 FUZZY COMPLEMENTS

Let A be a fuzzy set on X. Then, by definition, A (x) is interpreted as the degree to which x belongs to A. Let  $cA$  denote a fuzzy complement of A of type c. Then,  $cA(x)$  may be interpreted not only as the degree to which x belongs to  $cA$ , but also as the degree to which x does not belong to A. Similarly,  $A(x)$  may also be interpreted as the degree to which x does not belong to  $cA$ .

As a notational convention, let a complement  $cA$  be defined by a function

$$c : [0, 1] \rightarrow [0, 1],$$

which assigns a value  $c(A(x))$  to each membership grade  $A(x)$  of any given fuzzy set A. The value  $c(A(x))$  is interpreted as the value of  $cA(x)$ . That is,

$$c(A(x)) = cA(x) \text{ for all } x \in X \text{ by definition.}$$

Given a fuzzy set A, we obtain  $cA$  by applying function c to values  $A(x)$  for all  $x \in X$ , where function c is totally independent of elements x to which values  $A(x)$  are assigned; it depends only on the values themselves.

### 1.8.4 FUZZY INTERSECTION

The intersection of two fuzzy sets A and B is specified in general by a binary operation on the unit interval; that is, a function of the form

$$i : [0, 1] \times [0, 1] \rightarrow [0, 1],$$

For each element  $x$  of the universal set, this function takes as its argument the pair consisting of the element's membership grades in a set  $A$  and in set  $B$ , and yield the membership grade of the element in the set constituting the intersection of  $A$  and  $B$ . Thus,

$$(A \cap B)(x) = i[A(x), B(x)]$$

for all  $x \in X$ .

### 1.8.5 FUZZY UNIONS

Fuzzy unions are closely parallels that of fuzzy intersections. Like fuzzy intersection, the general fuzzy union of two fuzzy sets  $A$  and  $B$  is specified by a function

$$u : [0, 1] \times [0, 1] \rightarrow [0, 1].$$

The argument to this function is the pair consisting of the membership grade of some element  $x$  in fuzzy set  $A$  and the membership grade of that same element in fuzzy set  $B$ . The function returns the membership grade of the element in the set  $A \cup B$ . Thus,

$$(A \cup B)(x) = u[A(x), B(x)]$$

for all  $x \in X$ .

### 1.8.6 MEMBERSHIP FUNCTIONS

A membership function (MF) is a curve that defines how each point in the input space is mapped to a membership value (or degree of membership) between 0 and 1. The function  $\mu$  often be referred to as the “membership function” of the corresponding fuzzy set. It becomes apparent that classical sets are particular cases of fuzzy sets (where  $[0,1]$  is restricted to  $\{0,1\}$ ). Statements like “ $x$  is between 3 and 5” are called rigid meanwhile those like “ $x$  is near 4” are called flexible (Fig.1.9).

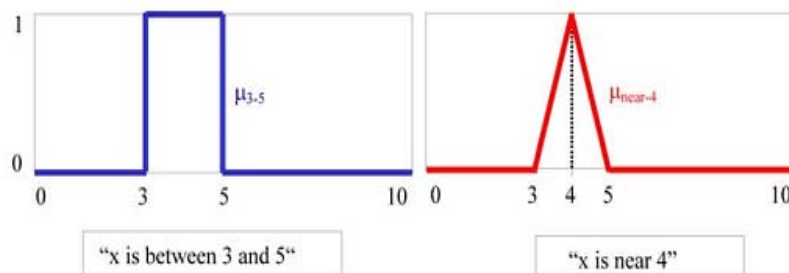


**Figure 1.9 Representation of rigid (left) and flexible (right) statement.**

The input space is sometimes referred to as the universe of discourse, a fancy name for a simple concept.

#### 2.1 CUTTING FORCE

**Latha & Senthilkumar (2009) [6]** deployed fuzzy rule-based model to predict the thrust force in drilling of GFRP composites. The machining parameters considered for the experiments were spindle speed, feed rate, and drill diameter. It was found that feed rate and drill diameter are the factors that influence the thrust force in drilling of GFRP composites. Furthermore spindle speed shows only very limited effect on thrust force. Their study reveals that the fuzzy rule-based model is better than the response surface model for predicting the thrust force in drilling of GFRP composites.

**Rajmohan and Palanikumar (2011) [7]** investigated the effect of thrust force in the drilling of hybrid MMCs using coated carbide drills. Materials used for the present investigation were Al 356-aluminum alloy reinforced with silicon carbide of size 25 microns and mica of an average size 45 microns, which were produced through stir casting route. Experiments were conducted on a vertical machining centre. The developed model was significant at 95% confidence level within the limits of parameters studied. The variance analysis it was concluded that the feed rate and wt% of SiC are the dominant factors which influence the thrust force of Al 356/SiC-mica composites. Through the analysis of the drilled surface of Al 356/SiC-mica composites it was found that some of the reinforcing SiC and mica particles are pulled out of the drilled surface, while others become cracked. Moreover, voids and cracks initiate around the particles due to plastic deformation in the matrix material.

**Haber et.al. (2009) [8]** made implementation of a neurofuzzy system for modeling and control of a high-performance drilling process in an Ethernet based application. The main goal was to keep constant the drilling force through real time control. Experimental trials were conducted using a Kondia HS1000 milling machine equipped with an open-CNC Sinumerik 840D controller. In the experiments a Sandvik R840-1000-30-A0A integral hard metal 10 mm diameter tool coated with TiN/TiAlN was used. The system was successfully applied to networked control of the high-performance drilling process. It was found that ANFIS-IMC control system yields an excellent dynamic response and therefore eliminates the risk of rapid tool wear and catastrophic tool breakage.

**Gajate et.al. (2010) [9]** applied a novel transductive neuro-fuzzy inference method to control force in a high-performance drilling process. Different drilling tests were conducted on A564

precipitation-hardening stainless steel test pieces. A control strategy based on the transductive neuro-fuzzy system and the IMC paradigm was proposed and applied to drilling force regulation. The transductive neuro-fuzzy inference system was also found to be a simple, fast, precise, and computationally viable tool for modeling and controlling the process. It was concluded that the transductive neuro-fuzzy control system provides a good transient response (without overshoot) and better error-based performance indices than the ANFIS-based control system.

**Krishnamoorthy et.al. (2010) [10]** developed a thrust force model in Drilling of CFRP composites using ANFIS. The input machining parameters considered were spindle speed, point angle and feed and the output parameter obtained was thrust force. The type of membership functions were chosen by trial and error and hence four types of membership functions namely, generalized bell shaped MF, triangular MF, Gaussian MF and two-bell Gaussian MF were applied. A 'Hybrid' parameter optimization method was chosen and the number of epochs for ANFIS training was 40. It was observed and concluded that adaptive neuro technique produced accurate prediction and thereby an accurate model. The performance factors used for evaluation of ANFIS results were namely, RMSE, MAE and R-Squared values, which were calculated for various number of training epochs with accuracy of the order of  $10^{-4}$ .

**Haber et.al. (2010) [11]** focused on optimal tuning of fuzzy control systems using the cross-entropy precise mathematical framework. Design of an optimal fuzzy controller for cutting force regulation in a network-based application was applied to the drilling process. The experimental results corroborate that the proposed optimal fuzzy control provides outstanding transient response without overshoot, a small settling time and a minimum of steady-state error. It was found that optimal fuzzy controller reduces the influence of the increasing cutting force that occurs as the drill depth increases, which can produce rapid drill wear and catastrophic drill breakage.

## 2.2 TOOL WEAR

**Patra et.al. (2007) [12]** developed a drill wear monitoring system which was independent to cutting conditions of the drilling process. An advanced signal processing technique, the wavelet packet transform was used on the acquired current signature to extract features for indirect representation to the amount of drill wear. The effects of variations of tool material and workpiece material was not considered in this analysis. It was observed that in comparison to time domain features, wavelet packet features are more sensitive to flank wear and less sensitive to the cutting conditions. A multilayer neural network model was developed to correlate the extracted wavelet packet features with drill flank wear with acceptable accuracy.

**Iqbal et.al. (2007) [13]** presented two fuzzy rules based strategies which compared accurate estimation of tool's flank wear in hard milling process. The offline strategy utilizes length of cut as major input while offline strategy uses force signals and found online strategy was 67.9% more accurate than offline one in estimating flank wear. It was concluded that cutting force

signals give better real time information about condition of in-progress machining process, whereas, length of cut does not possess such ability. Also Online strategy, using cutting force signals as primary input, gives better estimation of tool wear as compared to offline strategy that utilizes length of cut as primary input. The workpiece material used was AISI D2 having dimensions 100 mm × 33 mm × 33 mm.

**Panda et.al. (2008) [14]** used two different types of artificial neural network (ANN) architectures viz. back propagation neural network (BPNN) and radial basis function network (RBFN) to predict flank wear in drills. Drilling operations were conducted over a wide a range of cutting condition. Spindle speed was varied in the range 250–500 rpm in four steps. Feed rate was varied from 0.13 to 0.36 mm/rev in four steps. High-speed steel drills of four different diameters of (9, 10, 11 and 12 mm) have been used for drilling through holes of 15 mm thickness in cast iron plates. Different combinations of three design variables viz. Spindle speed, feed rate and drill diameter was used to perform 64 different drilling operations on cast iron plate. For each of these conditions, thrust force and torque was measured using dynamometer and the data was stored in the computer. Taking vibration signals as input to train neural network it was concluded that BPNN can predict the wear more accurately compared to RBFN. While RBFN can learn the pattern much faster compared to BPNN and could be used advantageously in online tool wear monitoring.

**Huseyin et.al. (2003) [15]** monitored drill wear using cutting force signals. Their Experimental results show that the reliability of the proposed methods. The use of HMM seems to have agree as a real time and data trainable system that does not require any mechanical and/or mathematical model of the machine tool. Because both the shape and amplitude of the force signals vary with tool wear, HMM is effective in comparing the data signals during the drilling operation. Moreover, the proposed HMM methods can be implemented on-line since the computation of the probabilities which indicate the status of tool wear can be performed during the non cut time between two consecutive drilling operations.

**A. Velayudhama, et.al. (2004) [16]** observed the dynamics of drilling of high volume fraction glass fibre reinforced composite since at high fibre volume, fibres do not show much relaxation and normal hole shrinkage associated with polymeric composites is not observed during drilling. Peak drilling thrust, dimension of holes drilled and vibration induced during drilling were observed to correlate with each other. Vibrations study was also attempted through wavelet packet transform and it was found that they are able to distinguish time–frequency information about tool cutting conditions. With higher cutting speed and feed (80.4 m/min and 315 mm/min) lower order peak thrust and torque were monitored. Only a marginal variation in thrust and wear occurs with 80.4 m/min of cutting speed and 400 mm/min.

**Alper Uysal et.al. (2012) [17]** applied Taguchi design of experiments and analysis of variance to determine the optimal cutting parameters and to analyze the effects of them on the tool wear. Drill point angle, feed, and cutting speed were chosen as key factors to be observed. The feed

followed by the drill point angle were found to be the important factors while cutting speed was the least effective parameter. They observed that tools with 80° drill point angle worn less than the others with 100° and 120° drill point angles. Multivariable linear regression analysis was also employed to determine the correlations between the factors and the tool wear.

**D. Ilescu et.al. (2010) [18]** developed a phenomenological model between the thrust force, the drilling parameters and the tool wear. The experimental results indicated that the feed rate, the cutting speed and the tool wear are the most significant factors affecting the thrust force. The model can then be used for tool-wear monitoring. The model was verified by experimental tests.

**Issam Abu-Mahfouz (2003) [19]** compared several architectures of the multi-layer feed-forward neural network with a back propagation training algorithm for tool condition monitoring (TCM) of twist drill wear. The algorithm utilizes vibration signature analysis as the main and only source of information from the machining process. The objective of the proposed study was to produce a TCM system that will lead to a more efficient and economical drilling tool usage. Five different drill wear conditions were artificially introduced to the neural network for prediction and classification. The experimental procedure for acquiring vibration data and extracting features in both the time and frequency domains to train and test the neural network models were detailed. It was found that the frequency domain features, such as the averaged harmonic wavelet coefficients and the maximum entropy spectrum peaks, are more efficient in training the neural network than the time domain statistical moments. The results demonstrate the effectiveness and robustness of using the vibration signals in a supervised neural network for drill wear detection and classification.

**S.S.Panda et.al. (2006) [20]** deployed a model for prediction of flank wear of drill bit using back propagation neural network (BPNN). Drilling operations were performed in mild steel work-piece by high-speed steel (HSS) drill bits over a wide range of cutting conditions. Important process parameters have been used as input for BPNN and drill wear has been used as output of the network. Inclusion of chip thickness as an input in addition to conventional parameters leads to better training of the network. Performance of the neural network has been found to be satisfactory while validated with experimental result. It has also been observed that inclusion of chip thickness as input to the neural network not only reduces mean square training error but also it is achieved at a much less number of iteration.

### **2.3 OPTIMIZATION OF PROCESS PARAMETER**

**Kilickap & Huseyinoglu (2010) [21]** deployed response surface methodology (RSM) and genetic algorithm (GA) for selecting the optimum combination values of drilling parameters affecting the burr height in drilling of AISI 304 stainless steel. Their study showed that it is possible to join together RSM (Box–Behnken design) with GA for the determination of close to optimal values in response surface design. RSM and GA approach provide a systematic and effective methodology for the modelling and the optimization.

**Wang et.al. (2011) [22]** developed optimization strategy and the associated software module for selecting the economic cutting conditions for drilling operations using the PRF drills. Optimization analysis assisted by graphical representations on the feed-speed domain was with consideration of deeper understanding of the economic characteristics and the influence of the constraints and machining performance data, which resulted in a clearly defined optimization strategy.

## **2.4 SURFACE ROUGHNESS**

**Latha and Senthilkumar (2010) [23]** applied fuzzy logic rule-based modeling and ANOVA analyses for modeling and analyzing the drilling of composite materials. The experiments were conducted on a computer numeric control drilling machine. The data for surface roughness were collected under different cutting conditions for various combinations of spindle speed, feed rate, and drill diameter. In fuzzy rule-based modeling, it was observed that the trapezoidal membership functions perform better than triangular membership functions. The results revealed that feed rate and drill diameter are the factors that influence the surface roughness in drilling of GFRP composites. Spindle speed shows only a limited effect on delamination in drilling of GFRP composites. The interaction between feed rate and drill diameter also shows some effect in drilling of composite materials.

**Nandi, and Davim (2009) [24]** studied the prediction of machining performances with Minimum Quantity of Lubricant in Drilling using Fuzzy Logic Rules aiming health and safety of operator, cost, ease of chip recyclability, etc. Two different types of fuzzy logic rules and two different shapes of MFDs were used to construct FRBMs in order to predict surface roughness, cutting power and specific force requirement in drilling of Aluminium AA1050. Four different FRBMs were developed using various methodologies in order to design optimal rule base and MFDs by adopting GA and Linear regression techniques. It was revealed that FRBM with TSK-type FLR and trapezoidal MFDs outperforms than other model in surface roughness prediction. While in cutting power and specific cutting force predictions, FRBM with TSK-type FLR and trapezoidal as well as second order polynomial MFDs provides best result than FRBM with Mamdani type FLR. It was concluded that for a constant cutting speed, the rate of change of surface quality with flow rate is minimized as feed rate increase. It was also found that for fixed values of cutting speed and feed rate, the cutting power increase to a certain value of lubrication flow rate. After that the value of cutting power decreases with increasing flow rate. Furthermore, constant cutting speed, the cutting power/specific force requirement increases with feed rate as well as with cutting speed when feed rate was kept as a constant value.

**K. Palanikumar (2010) [25]** modeled the delamination factor and surface roughness in machining of GFRP composites through response surface methodology. Three-factors five-levels central composite design was employed for carrying out this work. The results of analysis of variance indicated that the developed models are adequate at 95% confidence level within the limits of factors being considered. The influences of different parameters in drilling GFRP

composite have been analyzed in detail. The drilling parameters considered for the experiments were spindle speed, feed rate, and drill diameter. From the parameter studied, feed rate was the factor which have greater influence on delamination factor and surface roughness in drilling of GFRP composites. Drill diameter was found have very good influence on deciding the delamination factor in drilling of GFRP composites. For surface roughness, drill diameter have less influence than feed rate considered.

## 2.5 DELAMINATION

**C.C. Tsao (2005) [26]** studied the effect of effect of pilot hole on delamination when core drill drilling composite materials. An analytical approach to identifying the pilot hole between drill diameter ( $\eta$ ) and inner uncut portion ( $\gamma$ ) for delamination free drilling based on linear elastic fracture mechanics was derived in their study. The prediction of the model agreed quantify with the experimental results. Experimental results indicated that critical thrust force is reduced with pre-drilled pilot hole, while the drilling thrust is largely reduced by removal of chip effect.

**C.C. Tsao and H. Hocheng (2007) [27]** investigated the effect of tool wear on delamination in drilling composite material. The critical thrust force at the onset of delamination for worn drill were predicted and compared with that of ideal drill. The experimental results demonstrate that though the critical thrust force is higher with increasing wear ratio, the delamination becomes more liable to occur because the actual thrust force increases to larger extent, as the thrust factor ( $Z$ ) illustrates. Compared to sharp drill, the worn twist drill allows for lower feed rate below which the delamination damage can be avoided.

**Ali Faraz et.al. (2009) [28]** applied a new approach in unveiling and introducing the cutting edge rounding (CER) – a latent wear characteristic as a measure of sharpness/bluntness – of uncoated cemented carbide tools during drilling CFRP composite laminates. Four different types of drills (conventional and specialised) were tested to assess the applicability and relevance of this new wear feature. Mechanical loads (drilling thrust and torque) were recorded, and the hole entry and exit delamination were quantified. For the utilised tools, the accruing magnitude of CER was also recorded, in parallel with studying their conventional flank wear. Very appreciable correlations between the CER and the drilling loads, and also the quantitative delamination results were observed. Results reveal that this new wear type develops almost similarly for the selected tools and is practically independent of their respective conventional flank wear patterns. Moreover, a distinct, non-zero magnitude of the CER for a very fresh tool state may provide researchers with some lucid information in further studying the results during wear tests, more emphatically.

## CHAPTER 3

### EXPERIMENTATAION

---

#### 3.1 INTRODUCTION

Experimentation includes the various step involved in designing, conducting and analyzing an experiment. Various major step involved in this process are [29].

- Selection of factor and/or interactions to be evaluated
- Selection of number of levels for the factors
- Selection of appropriate OA
- Assignment of factors and/or interactions to column
- Conduct tests
- Analyze results
- Confirmation experiment

#### 3.2 DRILLING MACHINE

Drilling machine chosen for experimental work was an ENERGY made radial drilling machine, which is present in NON – TRADITIONAL MACHINING LAB of Thapar Uuniversity. Technical specification of drilling machining are given below.

**Table 3.1 Technical specification of drilling machining**

Sr. No.	Specification	Value
1	Speed	80, 122, 160, 244, 290, 445, 580, 890
2	Feed	0.1(fine), 0.15(coarse), manual
3	Amps.	2.25/3
4	H.P.	1.3/1.8

### 3.3 WORKPIECE

Work piece taken for experiment was GFRP. A 10 mm thick sheet was taken which later cut down into  $11 \times 11 \text{ cm}^2$  pieces. Matrix for composite was epoxy resin in which glass was reinforced. Another technical specification of material are tabulated below.

**Table 3.2 Properties of W/P material**

Properties	Unit	Value
Density	$\text{g/cm}^3$	1.70 – 1.90
Bending strength	$\text{kgf/cm}^2$	4000 - Longitudinal 3000 - Horizontal
Tensile strength	$\text{kgf/cm}^2$	3500 - Longitudinal 2500 - Horizontal
Impact strength (Charpy)	$\text{kJ/m}^2$	33
Flexural strength	MPa	340



**Figure 3.1 GFRP plate (Source-Internet)**

### 3.4 TOOL

Tool used for this work were of HSS. Drill of three different point angle and drill diameter were taken. So total of nine drill were used as shown in figure below.



**Figure 3.2 Drill bits ( Source - NTM-LAB, TU)**

### 3.4 DOE

In this phase different factor and their level of interest were selected that may consider that they will influence the drilling system. Selection of suitable OA and interaction all were selected in this phase. Different factors and their level taken for experimental work are tabulated below.

**Table 3.3 Factors and their levels**

FACTORS	LEVELS		
	Level-1	Level-2	Level-3
Feed (mm/rev)	0.1	0.15	-
Speed (rpm)	290	580	890
Drill diameter (mm)	6.0	7.1	9.1
Point angle (digree)	78	98	118

DOF of factors and interaction is calculated as shown below

Dof for any factor (say A)=  $k-1$

Where

$k$  = level of factor (A)

dof for any interaction ( say  $A \times B$  ) =  $(k_A-1) \times (k_B-1)$

where

$k_A$  = level of factor (A)

$k_B$  = level of factor (A)

in the present case as there are four factor and one first order interactions. Out of four factors one factor have only 2 level so it have one dof and other remaining three factor have 3 level each so each have 2 dof . so factors itself have 7 dof. One interactions have 2 dof . So their total dof becomes 9 as shown in table below.

**Table 3.4 Calculation of DOF**

Factor	Feed	Speed	Drill diameter	Point angle	Feed × Speed	Total
DOF	1	2	2	2	2	9

### 3.5 ORTHOGONAL ARRAY

As shown above total DOF for the experiment is 9 so an OA chosen for experimentation must have dof grater than 9 .  $L_{18}$  OA was found perfect for this case, so was taken. Table for  $L_{18}$  OA in coded form taken for experimentation is shown below

**Table 3.5  $L_{18}$  OA**

Runs	Factors			
	A	B	C	D
1	1	1	1	1
2	1	1	2	2
3	1	1	3	3
4	1	2	1	1
5	1	2	2	2
6	1	2	3	3
7	1	3	1	2
8	1	3	2	3

9	1	3	3	1
10	2	1	1	3
11	2	1	2	1
12	2	1	3	2
13	2	2	1	2
14	2	2	2	3
15	2	2	3	1
16	2	3	1	3
17	2	3	2	1
18	2	3	3	2

### 3.6 DRILLING PROCESS

First of all GFRP plate was cut down into small pieces of each  $11 \times 11 \text{ cm}^2$ . After that 2 hole at exact position was made to hold the workpiece on dynamometer. Drill bit were also prepared by own for that gages were made first for measuring angle. The schematic of drilling process is shown below.

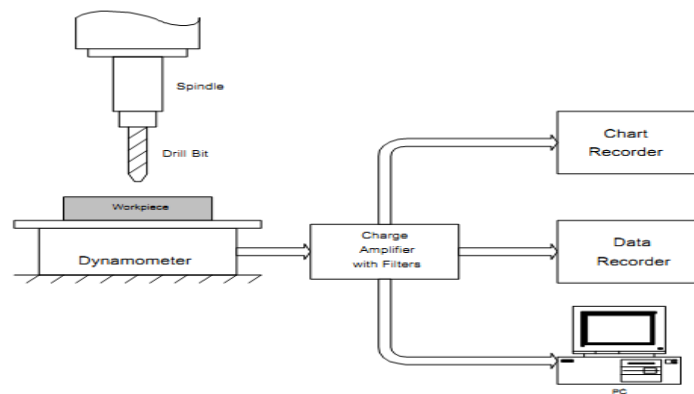


**Figure 3.3 Schematic of drilling process [19]**

After that machining of composite was done as per L18 OA trial run condition. Cutting forces in different direction were also measured using dynamometer (KISTLER, TYPE-9272) which was attached to computer. Data for the first trial run is shown below.

**Table 3.6 Drilling force table for 1 trial run**

<b>Parameter</b>	<b>Feed (mm/rev.)</b>	<b>Speed (rpm)</b>	<b>Drill diameter (mm)</b>	<b>Point angle (degree)</b>
Run - 1	0.1	290	6	78

File Type:				
Path:	C:\Kistler\DynoWare\			
Filename:	messdat.dwd			
Config ID:	messdat.cfg			
Setup ID:	0			
Manipulated:	0			
Filename 1:				
Filename 2:				
Date:				
Time:				
Sampling rate [Hz]:	2			
Measuring time [s]:	22			
Delay time [s]:	0			
Cycle time [s]:	0			
Cycles:	1			
Samples per channel:	45			
Cycle interval:	0			
Channel enabled:	1	1	1	1
Cycle No:	1			

<b>Time (s)</b>	<b>F<sub>X</sub> (N)</b>	<b>F<sub>Y</sub> (N)</b>	<b>F<sub>Z</sub> (N)</b>	<b>Torque (Nm)</b>
0	7.32E-02	0.32959	1.83E-02	0.177002
0.5	0.183105	0.3479	7.93E-02	-2.44E-02
1	3.66E-02	0.402832	0.109863	0.195313
1.5	0.189209	0.506592	0	-6.10E-03
2	1.22E-02	0.622559	9.77E-02	0.219727
2.5	0.274658	0.57373	-6.10E-03	6.10E-03
3	2.44E-02	0.622559	0.244141	0.128174
3.5	0.177002	0.622559	-4.27E-02	7.32E-02
4	6.10E-02	0.543213	0.10376	7.93E-02
4.5	0.109863	0.494385	-1.83E-02	8.54E-02
5	0.158691	0.421143	9.77E-02	-3.66E-02
5.5	0	0.43335	3.66E-02	0.20752
6	0.238037	0.482178	1.22E-02	-6.10E-03
6.5	7.32E-02	0.488281	0	0.22583
7	0.262451	0.488281	3.66E-02	-8.54E-02
7.5	4.88E-02	0.457764	0.158691	0.250244
8	0.256348	0.482178	-5.49E-02	1.22E-02
8.5	3.05E-02	0.402832	0.164795	0.134277
9	0.219727	0.341797	-0.12817	3.66E-02
9.5	7.93E-02	0.482178	6.10E-02	0.158691
10	0.140381	0.476074	-0.10986	0.146484
10.5	0.128174	0.543213	0.195313	2.44E-02
11	0.109863	0.665283	-2.44E-02	0.20752

11.5	0.22583	0.628662	0.140381	-3.66E-02
12	4.88E-02	0.616455	-2.44E-02	0.280762
12.5	0.292969	0.653076	1.22E-02	-2.44E-02
13	0	0.579834	4.27E-02	0.317383
13.5	0.256348	0.439453	-6.10E-02	-2.44E-02
14	-2.44E-02	0.543213	0.134277	0.299072
14.5	0.256348	0.457764	-4.27E-02	5.49E-02
15	-6.10E-03	0.415039	0.20752	0.274658
15.5	0.195313	0.408936	-8.54E-02	0.170898
16	6.10E-02	0.439453	0.286865	0.128174
16.5	0.10376	0.55542	6.10E-03	0.244141
17	0.195313	0.408936	0.238037	0
17.5	-6.10E-03	0.299072	3.66E-02	0.317383
18	0.262451	0.152588	0.12207	0
18.5	-1.22E-02	0.10376	9.77E-02	0.311279
19	0.256348	5.49E-02	1.22E-02	-6.10E-03
19.5	1.83E-02	6.10E-02	0.158691	0.250244
20	0.22583	0	-0.12817	9.77E-02
20.5	0	4.27E-02	0.177002	0.146484
21	0.170898	4.88E-02	-0.11597	0.238037
21.5	0.140381	-6.10E-03	0.183105	6.10E-02
22	-6.10E-03	7.32E-02	-4.88E-02	0.366211

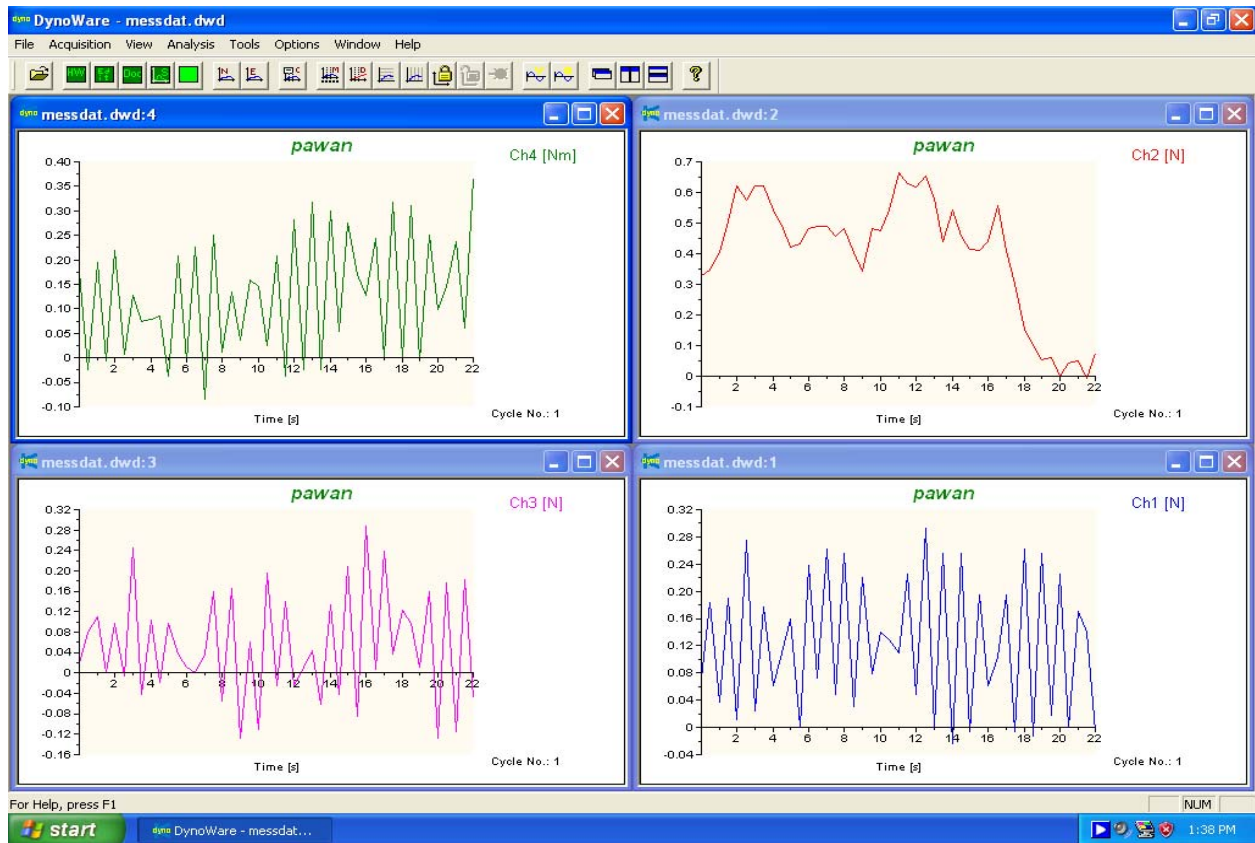


**Figure 3.4 Force plot for 1 trial run**

Similarly data for remaining run was collected. Average value of forces was taken for different trial run in consideration as shown in table below.

**Table 3.7 Drilling force table for all trial run**

Runs	$F_x$ (N)	$F_y$ (N)	$F_z$ (N)	Torque (Nm)
1	0.123155	0.404595	0.052897	0.126139
2	0.156569	0.38001	0.085184	0.128439
3	0.178971	0.41307	0.127386	0.229177
4	0.239702	0.352339	0.14371	0.208629
5	0.26757	0.56428	0.180546	0.268555
6	0.278542	0.486617	0.201416	0.330145
7	0.358344	0.966254	0.171034	0.290392

8	0.367803	0.944719	0.164264	0.2866
9	0.393195	0.54514	0.254741	0.330232
10	0.393473	0.532634	0.321045	0.432943
11	0.486354	0.529078	0.390946	0.465473
12	0.435791	0.519613	0.358887	0.594075
13	0.543077	0.814752	0.418701	0.646159
14	0.570015	0.834059	0.424062	0.630254
15	0.519762	0.97592	0.568269	0.749448
16	0.618083	0.940349	0.476888	0.720215
17	0.662509	1.083097	0.441673	0.706898
18	0.672765	1.221688	0.499898	0.770027

### 3.7 ANALYSIS OF RESULTS

After completing the experiment procedure the result were analyzed. The various factor or sources of variation which affect the system can be categorized as control (signal) and uncontrollable (noise). Control factor are those which are in control of designer means their level can be set and their effect on system can be analyzed. Noise factor are those factor which are out of control of designer. Various response characteristics which obtained through experimentation are categorized as tabulated below.

**Table 3.8 Various response characteristics**

<b>Sr. No.</b>	<b>Response Characteristic</b>	<b>Response Type</b>	<b>Units</b>
1	MRR	Higher is better	mm <sup>3</sup> /min
2	SR	Lower is better	Microns
3	TWR	Lower is better	mm

The various quality characteristics for S/N ratio are formulated below.

$$S/N = -10 \text{ Log (MSD)} \quad (\text{Eq. 3.1})$$

Where,

MSD = mean square deviation from the target value of the quality characteristics.

For Smaller is better

$$MSD = \frac{1}{n} \sum_{i=1}^n y_i^2$$

Nominal is better

$$MSD = \frac{1}{n} \sum_{i=1}^n (y_i - y_0)^2$$

Higher is better

$$MSD = \frac{1}{n} \sum_{i=1}^n \frac{1}{y_i^2}$$

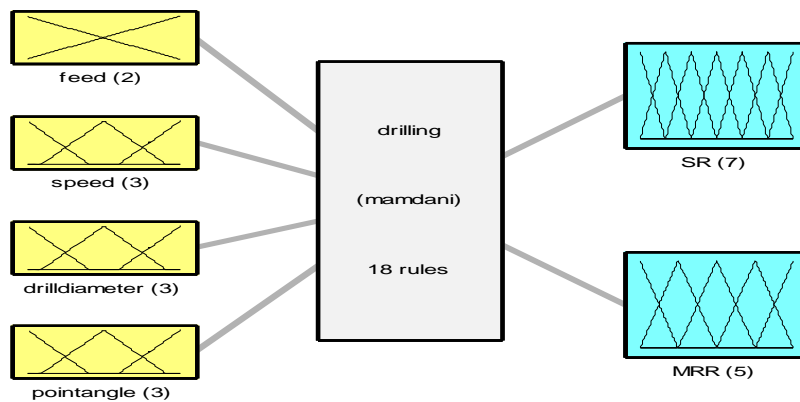
Where,

$y_1, y_2, \dots$  = quality characteristic

m = target value

n = number of repetitions

After that fuzzy model was prepared. A MIMO system was used. Mamdani inference system was used for modeling of drilling system. Configuration of system is shown in figure below.



System drilling: 4 inputs, 2 outputs, 18 rules

Two kind of membership function (triangular and trapezoidal) were used for modeling and their performance was compared.

**4.1 INTRODUCTION**

The effects of sources of variation (i.e. feed, speed, drill diameter and point angle) on different response characteristic was studied. A confidence interval of 95% has been used for the analysis. For assistance statistical software MINITAB-16 was used.

**4.2 RESULTS FOR MRR**

The results for MRR for each of the 18 runs are given in table below. MRR of each sample was calculated from weight difference of material removed with container and container for the each trial, which is given by:

$$MRR = \frac{w_1 - w_2}{\rho \times t}, \text{ cm}^3 / \text{s}$$

Where

$W_1$  = weight of material removed with container (gms)

$W_2$  = weight of container (gms)

t = time period of run in seconds

$\rho$  = Density of work piece in gms/cc

METTLE TOEDO, PB-303S modal weighing machine was used for weight measurement.

**Table 4.1 Trial results for MRR**

Runs	Feed (mm/rev.)	Speed (rpm)	Drill diameter (mm)	Point angle (degree)	MRR* (cm <sup>3</sup> /sec.)	S/N ratio (db)
1	0.1	290	6.0	78	0.02	-33.9794
2	0.1	290	7.1	98	0.04	-27.9588

3	0.1	290	9.1	118	0.06	-24.437
4	0.1	580	6.0	78	0.05	-26.0206
5	0.1	580	7.1	98	0.08	-21.9382
6	0.1	580	9.1	118	0.12	-18.4164
7	0.1	890	6.0	98	0.08	-21.9382
8	0.1	890	7.1	118	0.13	-17.7211
9	0.1	890	9.1	78	0.19	-14.4249
10	0.15	290	6.0	118	0.04	-27.9588
11	0.15	290	7.1	78	0.08	-21.9382
12	0.15	290	9.1	98	0.09	-20.9151
13	0.15	580	6.0	98	0.06	-24.437
14	0.15	580	7.1	118	0.10	-20
15	0.15	580	9.1	78	0.15	-16.4782
16	0.15	890	6.0	118	0.12	-18.4164
17	0.15	890	7.1	78	0.18	-14.8945
18	0.15	890	9.1	98	0.28	-11.0568

\* average of 2 readings

#### 4.2.1 ANOVA FOR MRR

The results for MRR were analyzed using ANOVA technique. The variance data for each factor and their interactions were tested to find either they are significance or not. F-statistic was used for that which a ratio of variance due to effect of a factor and variance due to error term. It can be concluded from table that speed, speed and drill diameter have F-value more than the F-critical or tabulated value so these are significant. As other factor have less F-value than F-critical so they have less influence on mean so they were pooled.

**Table 4.2 ANOVA for Means of MRR**

Sources of variation	SS	v	V	F	F(critical)	SS'	(%) P
Feed, A	0.00605	1	0.00605	11.0	5.32	0.00555	7.77
Speed, B	0.036211	2	0.01810	32.92	4.46	0.035211	49.30
Drill diameter, C	0.022578	2	0.11289	20.53	4.46	0.021578	30.21
Point angle, D	0.000844	2	0.00042	0.77	-	-	-
Feed × Speed, A×B	0.0013	2	0.00065	1.18	-	-	-
Error	0.004444	8	0.00055	-	-	-	-
Total	0.071428	17	-	-	-	-	-
e-pooled	0.006588	12	0.0005	-	-	0.009	12.72

**Table 4.3 Response Table for Means of MRR**

Level	Feed (mm/rev.)	Speed (rpm)	Drill diameter (mm)	Point angle (degree)
1	0.08556	0.055	0.06167	0.11167
2	0.12222	0.09333	0.10167	0.10500
3	-	0.16333	0.14833	0.09500
Delta	0.03667	0.10833	0.08667	0.01667
Rank	3	1	2	4

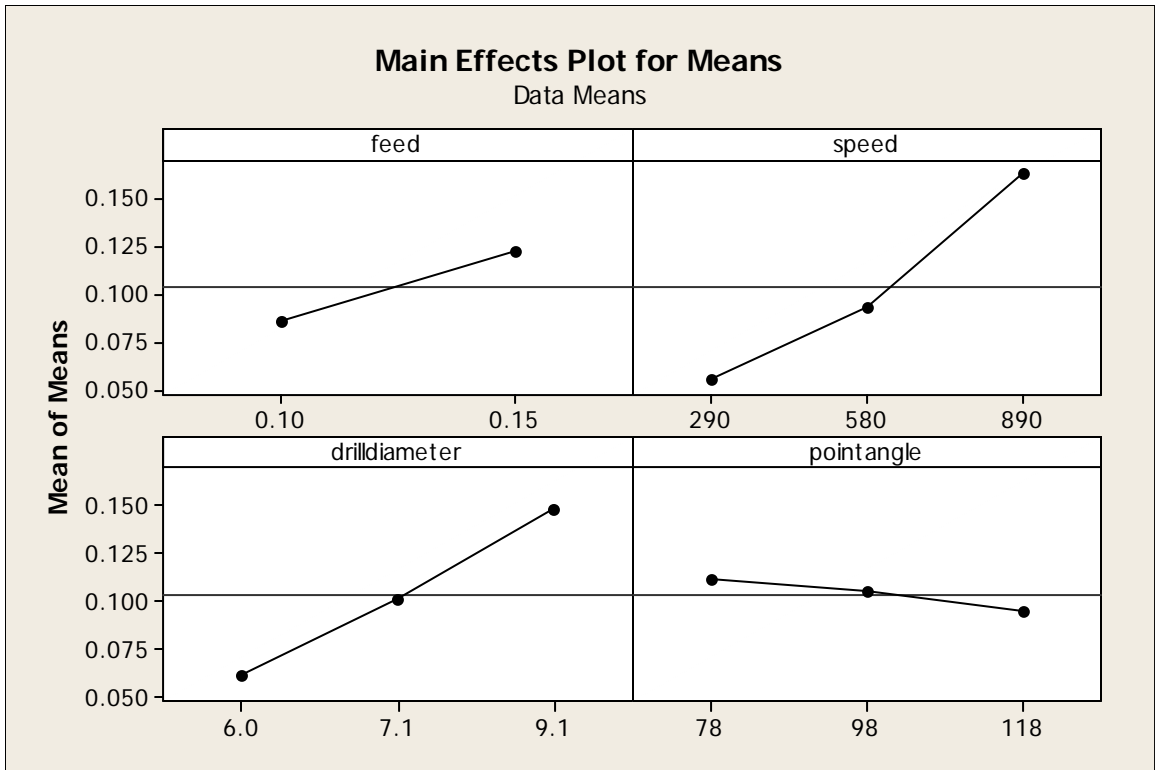


**Figure 4.1 Main effects plot for MRR**

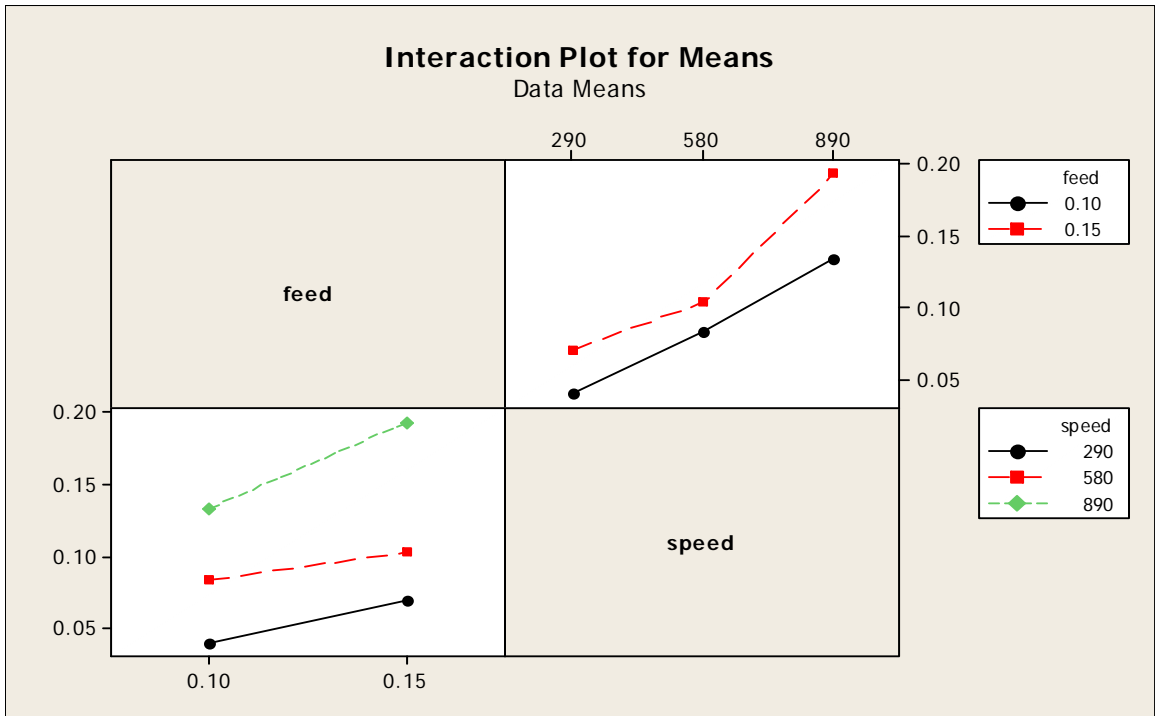


**Figure 4.2 Interaction plot for MRR**

#### 4.2.2 ANOVA FOR S/N RATIO OF MRR

The S/N ratio is an indication of the amount of variation present. The S/N ratios have been calculated to identify the major contributing factors and interactions that cause variation in the MRR. For MRR low MSD will be preferred. ANOVA table for S/N ratio of MRR is shown below. From table it can be found that feed, speed and drill diameter have higher F-value than F-critical hence are significant. An interaction between feed and speed is also significant.

**Table 4.4 ANOVA for S/N of MRR**

Sources of variation	SS	v	V	F	F(critical)	SS'	(%) P
Feed, A	52.496	1	52.496	86.90	5.32	86.4025	15.99
Speed, B	287.517	2	143.7585	239.62	4.46	286.522	53.02
Drill diameter, C	186.803	2	93.4015	154.60	4.46	185.808	34.39
Point angle, D	0.142	2	0.071	0.12	-	-	-
Feed × Speed , A×B	8.576	2	4.288	7.10	4.46	7.581	1.4
Error	4.833	8	0.6041	-	-	-	-
Total	540.367	17	-	-	-	-	-
e-pooled	4.975	10	0.4975	-	-	8.4575	1.57

**Table 4.5 Response table for S/N ratio of MRR**

Level	Feed (mm/rev.)	Speed (rpm)	Drill diameter (mm)	Point angle (degree)
1	-22.98	-26.20	-25.46	-21.29
2	-19.57	-21.22	-20.74	-21.37
3	-	-16.41	-17.62	-21.16
Delta	3.42	9.79	7.78	0.22
Rank	3	1	2	4

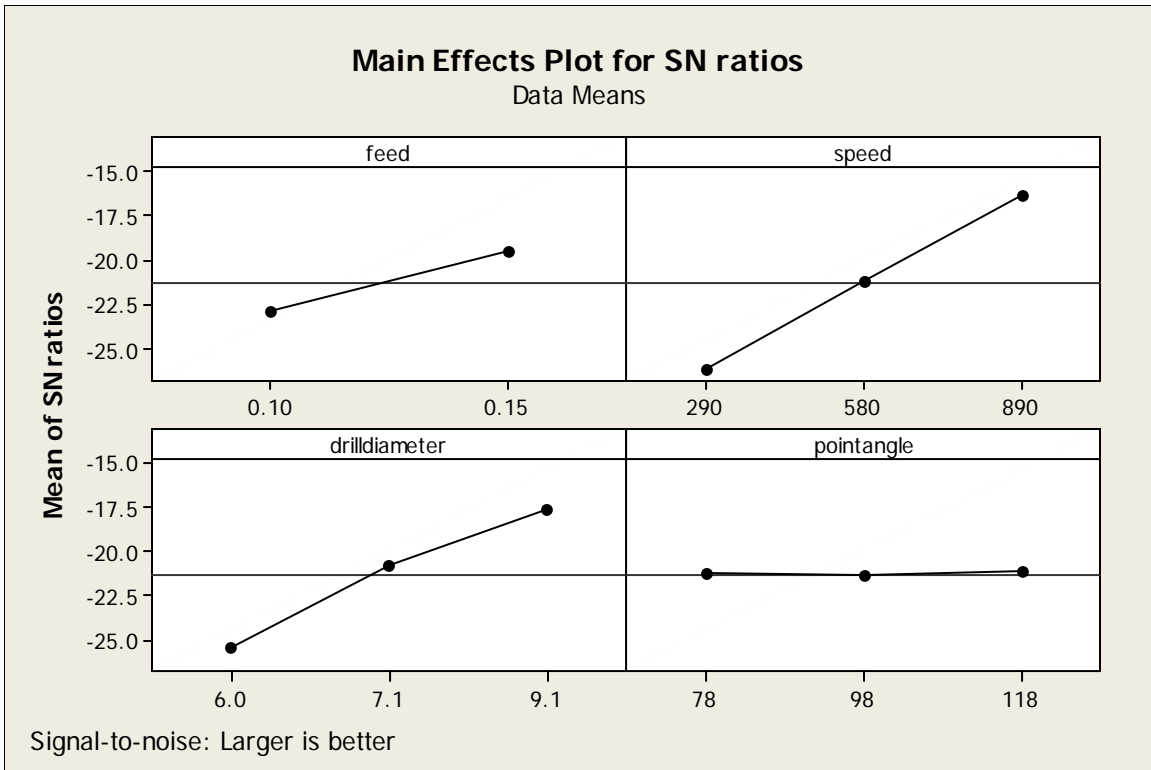


**Figure 4.3** Main effects plot of MRR for S/N ratio

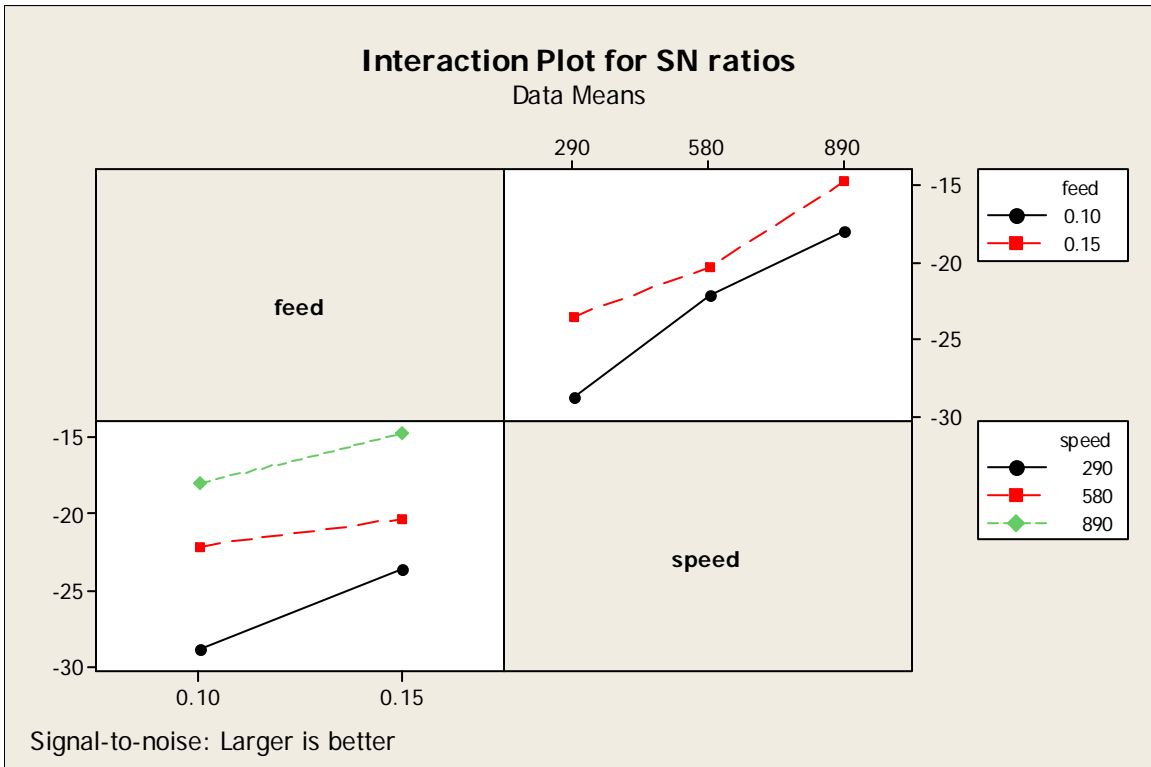


**Figure 4.4** Interaction plot of MRR for S/N ratio

### 4.2.3 OPTIMAL DESIGN FOR MRR

The table shown below is representing the combined result of both mean and variation of MRR. The different level of significant factors can be easily find out from their respective graph or plots. For means according to response characteristics higher or lower value/level is selected but for variance always higher value is preferred.

**Table 4.6 Significant factors and interactions**

Sources of variation	Affecting mean		Affecting variation	
	Contribution	Best level	Contribution	Best level
Feed, A	Significant	Level2 (0.15,mm/rev.)	Significant	Level-2 (0.15,mm/rev.)
Speed, B	Significant	Level-3 (890,rpm)	Significant	Level-3 (890,rpm)
Drill diameter, C	Significant	Level-3 (9.1,mm)	Significant	Level-3 (9.1,mm)
Point angle, D	Insignificant	-	Insignificant	-
Feed × Speed, A×B	Insignificant	-	Significant	A <sub>2</sub> ×B <sub>3</sub>

### 4.2.4 ESTIMATED RESULT AT OPTIMUM CONDITION

$$MRR = C_3 + \overline{A_2 \times B_3} - 2\overline{T}$$

$$= 0.14833 + 0.1933 - 2 \times 0.103889 = 0.133832 \text{ cm}^3/\text{sec} = 8029.92 \text{ mm}^3/\text{min}$$

### 4.2.5 CONFIDENCE INTERVAL OF RESULT AT OPTIMUM CONDITION

$$C.I. = \sqrt{\frac{F_{\alpha, v_1, v_2} \times V_e}{N_{eff}}}$$

Where

$\alpha$  = risk level (i.e. 0.05)

$F_{v_1v_2}$  = The F value at a required confidence level at DOF  $v_1$  error DOF  $v_2$

$$N_{eff} = N / (1 + DOF_{A,B,C})$$

$$= 18 / (1 + 1 + 2 + 2) = 3$$

$$C.I. = \sqrt{\frac{4.75 \times 0.0005}{3}} = 0.028$$

So the result at optimum condition is  $8029.92 \pm 0.028 \text{ mm}^3/\text{min}$ .

### 4.3 RESULTS FOR SURFACE ROUGHNESS

The results for SR were obtained by using surface roughness tester MITUTOYO, SJ-400 which is present in the metallurgical laboratory of Institute. A sampling length of 0.08mm and trace length of 3mm was taken for measurement. Results for SR for different trial runs are shown below.

**Table 4.7 Trial results for SR**

Runs	Feed (mm/rev.)	Speed (rpm)	Drill diameter (mm)	Point angle (degree)	SR* (microns)	S/N ratio (db)
1	0.1	290	6.0	78	0.29	10.7520
2	0.1	290	7.1	98	0.43	7.3306
3	0.1	290	9.1	118	0.37	8.6360
4	0.1	580	6.0	78	0.30	10.4576
5	0.1	580	7.1	98	0.51	5.8486
6	0.1	580	9.1	118	0.80	1.9382
7	0.1	890	6.0	98	0.38	8.4043
8	0.1	890	7.1	118	0.25	12.0412
9	0.1	890	9.1	78	0.39	8.1787
10	0.15	290	6.0	118	0.60	4.4370

11	0.15	290	7.1	78	0.74	2.6154
12	0.15	290	9.1	98	1.10	-0.8279
13	0.15	580	6.0	98	0.60	4.4370
14	0.15	580	7.1	118	0.50	6.0206
15	0.15	580	9.1	78	0.75	2.4988
16	0.15	890	6.0	118	0.54	5.3521
17	0.15	890	7.1	78	0.44	7.1309
18	0.15	890	9.1	98	0.96	0.3546

\* average of 2 readings

#### 4.3.1 ANOVA FOR SR

From the ANOVA of SR it was found that the only factor speed is insignificant and interaction between factors Speed and feed is also found significant as their F-value is larger than F-tabulated at a selected confidence level. Percentage contribution of different factor can also be notice from the table below.

**Table 4.8 ANOVA for Means of SR**

Sources of variation	SS	v	V	F	F(critical)	SS'	(%) P
Feed, A	0.35001	1	0.35001	38.04	5.32	0.33951	35.67
Speed, B	0.03221	2	0.016105	1.75	-	-	-
Drill diameter, C	0.27951	2	0.139755	15.19	4.46	0.25851	27.16
Point angle, D	0.11188	2	0.05594	6.08	4.46	0.09088	9.55
Feed × Speed, A×B	0.10441	2	0.052205	5.67	4.46	0.08341	8.76
Error	0.07374	8	0.0092	-	-	-	-
Total	0.95176	17	-	-	-	-	-
e-pooled	0.10595	10	0.0105	-	-	0.17945	18.85

**Table 4.9 Response Table for Means of SR**

Level	Feed (mm/rev.)	Speed (rpm)	Drill diameter (mm)	Point angle (degree)
1	0.4133	0.5883	0.4517	0.4850
2	0.6922	0.5767	0.4783	0.6633
3	-	0.4933	0.7283	0.5100
Delta	0.2789	0.0950	0.2767	0.1783
Rank	1	4	2	3

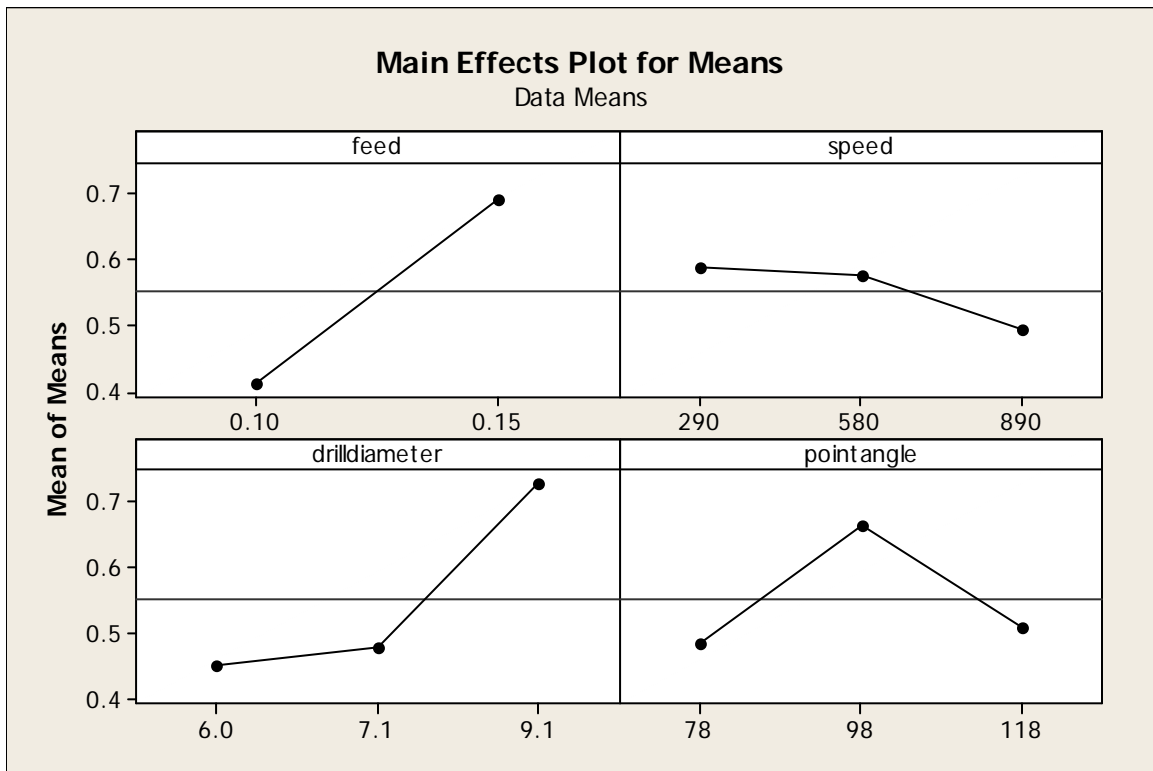


**Figure 4.5 Main effects plot for SR**

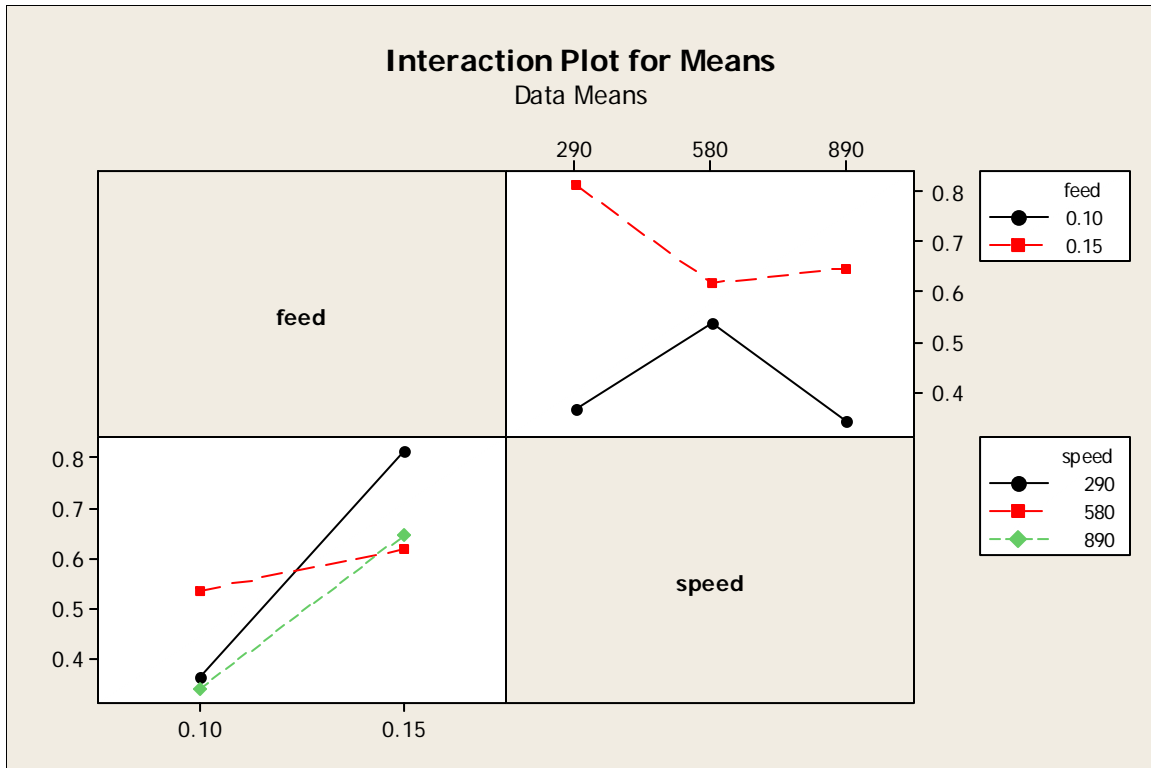


Figure 4.6 Interaction plot for SR

### 4.3.2 ANOVA FOR S/N OF SR

For SR high MSD value will be preferred because it is 'Lower is better' kind of characteristics. ANOVA table for S/N ratio of SR is shown below. From table it can be found that out of four factors only speed is insignificant and other have higher F-value than F-critical hence all are significant.

Table 4.10 ANOVA for S/N of SR

Sources of variation	SS	v	V	F	F(critical)	SS'	(%) P
Feed, A	96.00	1	96.00	38.23	5.32	92.65	41.51
Speed, B	10.05	2	5.025	2.00	-	-	-
Drill diameter, C	52.69	2	26.35	10.49	4.46	45.99	20.61
Point angle, D	24.16	2	12.08	4.81	4.46	17.46	7.82
Feed × Speed, A×B	20.20	2	10.10	4.02	-	-	-

Error	20.09	8	2.511	-	-	-	-
Total	233.19	17	-	-	-	-	-
e-pooled	40.24	12	-	-	-	56.99	25.54

**Table 4.11 Response table for S/N ratio of SR**

Level	Feed (mm/rev.)	Speed (rpm)	Drill diameter (mm)	Point angle (degree)
1	8.176	5.491	7.307	6.939
2	3.558	5.200	6.831	4.258
3	-	6.910	3.463	6.404
Delta	4.619	1.710	3.844	2.681
Rank	1	4	2	3

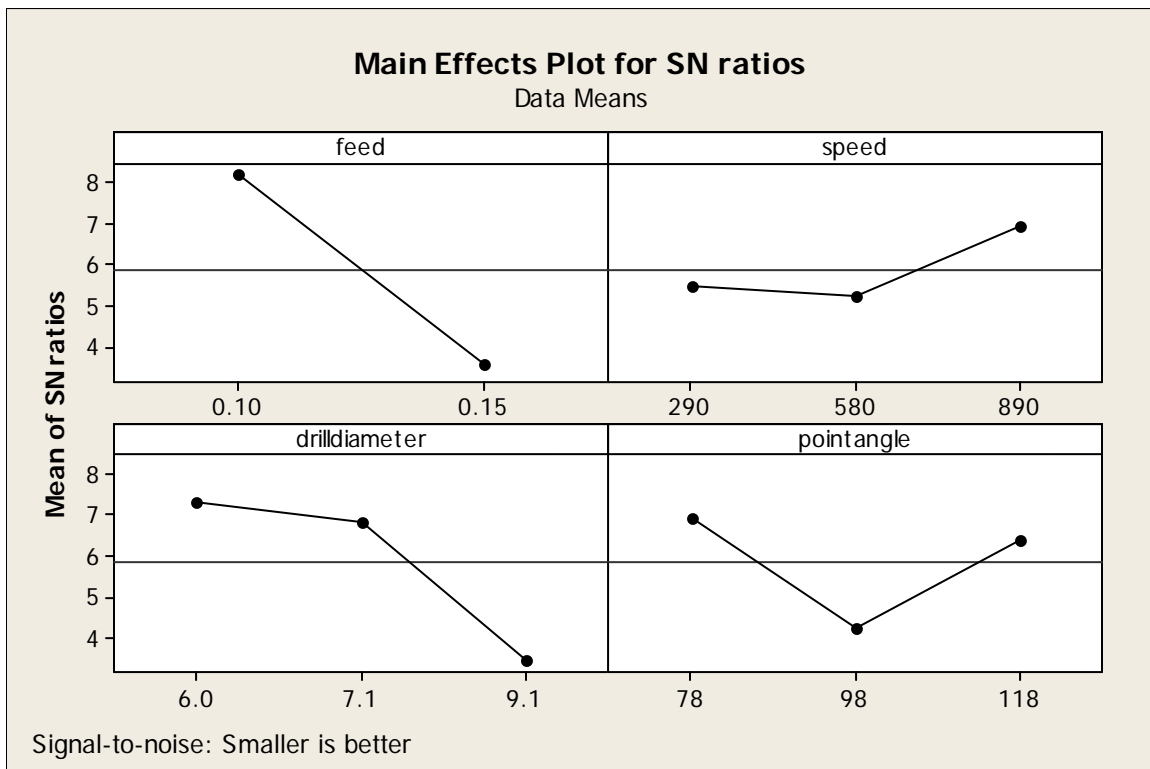


**Figure 4.7 Main effects plot of SR for S/N ratio**

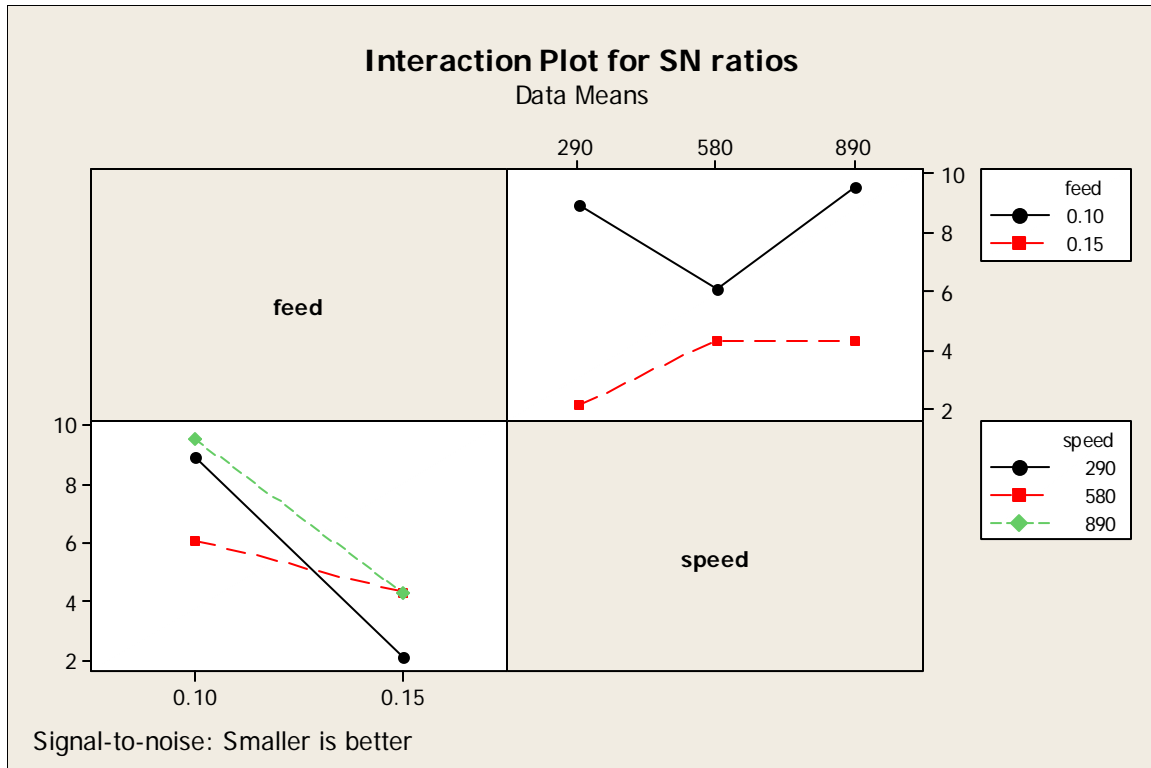


**Figure 4.8 Interaction plot of SR for S/N ratio**

### 4.3.3 OPTIMAL DESIGN FOR SR

By taking the consideration of tables shown above for mean and variance and their respective graphs it was asserted that feed & drill diameter with level-1 are significant and interaction of these with level 1 & 3 respectively is significant. But point angle with 1&3-level is significant according to means and variation respectively.

**Table 4.12 Significant factors and interactions**

Sources of variation	Affecting mean		Affecting variation	
	Contribution	Best level	Contribution	Best level
Feed, A	Significant	Level-1 (0.10. mm/rev.)	Insignificant	Level-1 (0.10. mm/rev.)
Speed, B	Insignificant	-	Insignificant	-
Drill diameter, C	Significant	Level-1 (6.0, mm)	Insignificant	Level-1 (6.0, mm)

Point angle, D	Significant	Level-3 (118 <sup>0</sup> )	Insignificant	Level-1 (78 <sup>0</sup> )
Feed × Speed, A×B	Significant	A <sub>1</sub> ×B <sub>3</sub>	Insignificant	-

#### 4.3.4 ESTIMATED RESULT AT OPTIMUM CONDITION

$$SR = \overline{C_1} + \overline{D_3} + \overline{A_1 \times B_3} - 2\overline{T}$$

$$= 0.7283 + 0.485 - 2 \times 0.5527 = 0.12 \mu\text{m}$$

#### 4.3.5 CONFIDENCE INTERVAL AROUND THE ESTIMATED MEAN

$$C.I. = \sqrt{\frac{F_{\alpha v_1 v_2} \times V_e}{N_{eff}}}$$

Where

$\alpha$  = risk level (i.e. 0.05)

$F_{v_1 v_2}$  = The F value at a required confidence level at DOF  $v_1$  error DOF  $v_2$ .

$N_{eff} = N / (1 + DOF_{A,B,C,D})$

$= 18 / (1 + 1 + 2 + 2 + 2) = 2.25$

$$C.I. = \sqrt{\frac{4.97 \times 0.0105}{2.25}} = 0.15$$

So the result at optimum condition is  $0.12 \pm 0.15 \mu\text{m}$ .

#### 4.4 TOOL WEAR

The results for TWR for each of the trial runs was measured by taking difference in weight of tool before and after drilling each hole. The following formula was used

$$TWR = \frac{w_1 - w_2}{\rho \times t}$$

where

$w_1$  = weight of drill bit after drilling

$w_2$  = weight of drill bit before drilling

$\rho$  = density of drill bit material

$t$  = machining time

METTLE TOEDO, PB-303S modal weighing machine was used for weight measurement. But no tool wear was found. Still to study the tool behavior by taking number of hole as drilling parameter drilling operation was performed. Flank wear was noticed for drill bit after each 10 hole. Table below showing the data of forces in three direction and torque value which was obtained through data acquisition system.

Tool wear reading were taken with the help of metallurgical microscope. A special arrange were made to observe the flank face. LEICA. DFC-280 metallurgical microscope was used for experimentation. Average of two edge reading was taken for consideration.

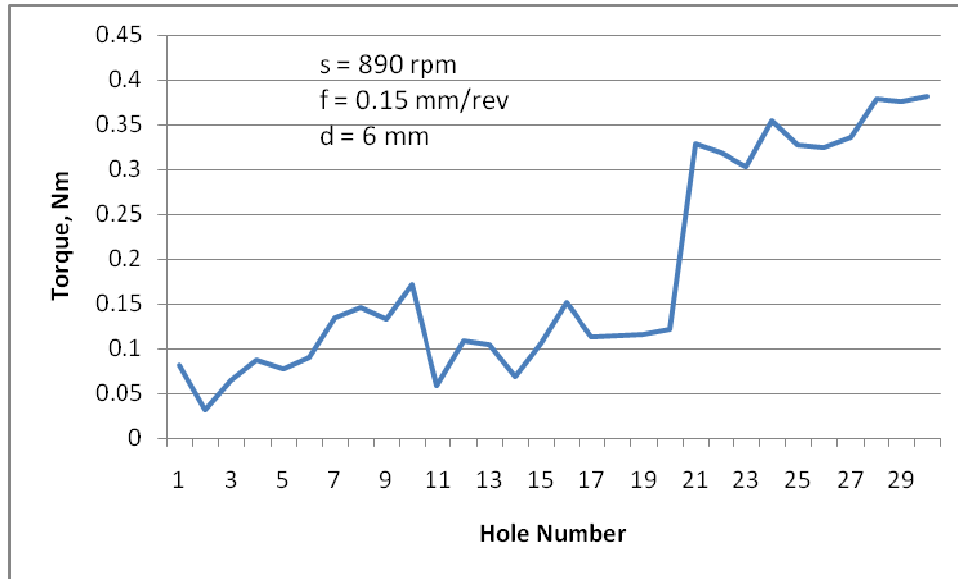
Table below is showing the data for 30 reading of forces and torque. The drilling operation was conducted at 890rpm at coarse feed with 6.0 mm HSS drill bit.

**Table 4.13 Force table for tool wear**

Hole No.	F <sub>x</sub> (N)	F <sub>y</sub> (N)	F <sub>z</sub> (N)	Torque (Nm)
1	-0.07269	1.338334	0.127064	0.081565
2	0.059371	1.063676	0.08434	0.032182
3	0.057706	1.114169	0.117631	0.064364
4	0.088778	1.164106	0.111528	0.088223
5	0.147594	1.138584	0.107089	0.078236
6	0.157582	1.142468	0.142046	0.090443
7	0.143155	1.160777	0.177002	0.134277
8	0.155917	1.209607	0.163685	0.147039
9	0.177002	1.145796	0.121516	0.133722
10	0.186435	1.29894	0.157582	0.172563

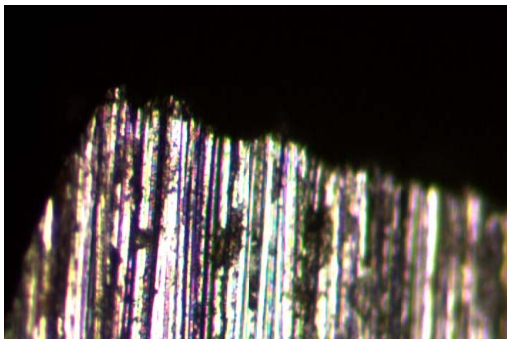
11	0.087669	1.039262	0.084894	0.058816
12	0.08323	0.940496	0.048273	0.109863
13	0.133723	1.013184	0.08212	0.10487
14	0.167569	0.906095	0.103205	0.068803
15	0.145375	1.017622	0.125399	0.106534
16	0.097656	0.982112	0.08323	0.151478
17	0.1254	1.096968	0.078236	0.113747
18	0.127619	1.116943	0.139826	0.115412
19	0.174782	1.074774	0.118186	0.116522
20	0.160911	0.971568	0.112083	0.121515
21	0.405051	1.685125	0.410045	0.32959
22	0.426136	1.593017	0.373979	0.318493
23	0.367875	1.513672	0.410045	0.303511
24	0.37176	1.547519	0.435569	0.354004
25	0.447221	1.40048	0.378418	0.32737
26	0.442227	1.394931	0.395064	0.324596
27	0.472745	1.631858	0.418368	0.335693
28	0.448331	1.521439	0.407271	0.379528
29	0.455544	1.460405	0.423362	0.376199
30	0.488836	1.493142	0.447776	0.381747

Figure below is presenting the torque variation with number of holes. From figure it can be concluded that increase value of torque is due to drill wear.

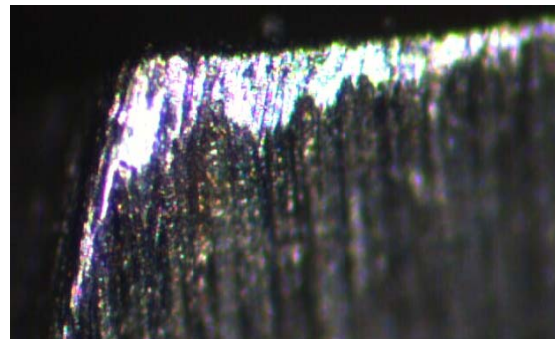


**Figure 4.9 Torque Vs Hole number**

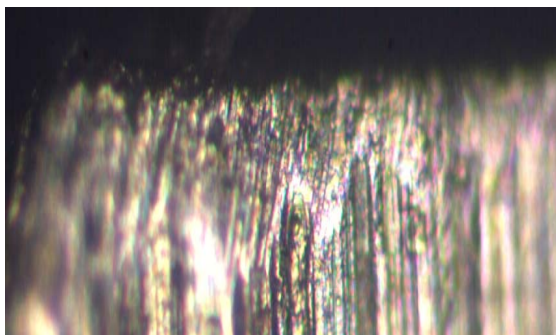
The graph below is showing the drill flank wear variation with number of hole. Flank wear ( $VB_C$ ) for drill was measured after drilling 10 hole each time. The variation of wear observed is shown in figure below.



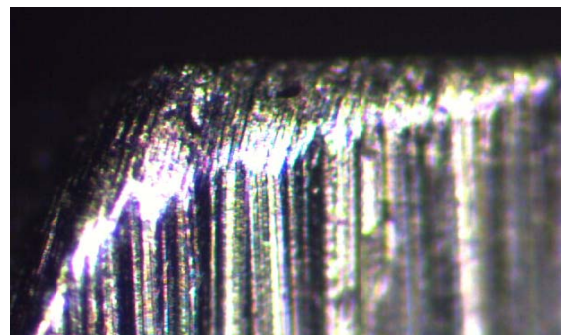
(a) No hole



(b) After 10 hole



(c) After 20 hole



(d) After 30 hole

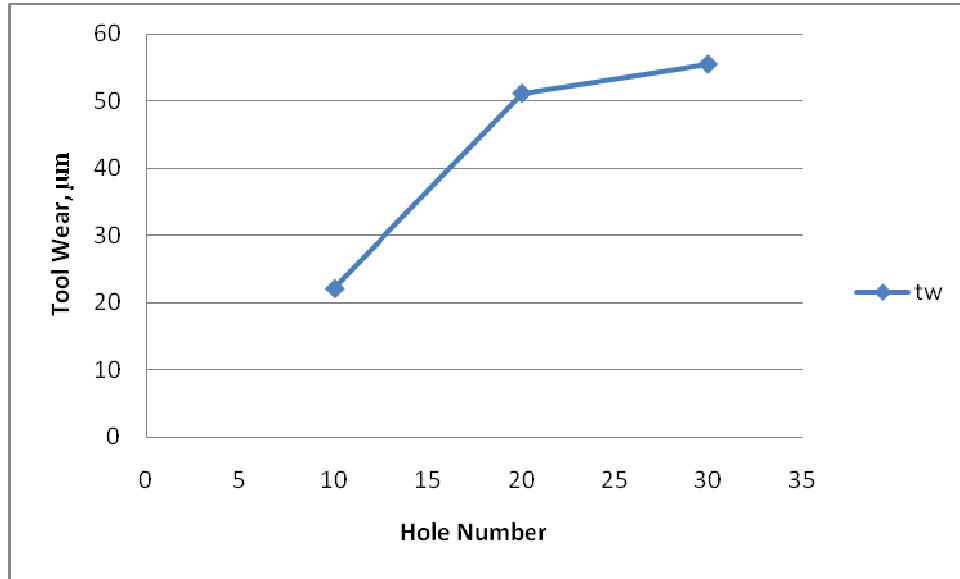


**Figure 4.10 Tool wear Vs Hole number (cutting condition,  $f = 0.15\text{mm/rev.}$ ,  $s = 890\text{rpm}$ ,  $d = 9.1\text{mm}$ )**

From plot it is clear that wear value is rapidly raised after doing 10 hole. At that time increase in length (b) was observed. The wear value for C- region was taken as per table given below.

**Table 4.14 Wear variation with number of hole**

Hole No.	0	10	20	30
VBc (mm)	-	22.148	51.22	55.55

**5.1 INTRODUCTION**

Fuzzy logic is an important methodology from AI and is an effective tool for dealing complex non linear system. Fuzzy modeling of present work was done in this chapter using fuzzy logic tool box. MATLAB software was used for this purpose. Fuzzy modeling of the drilling process was done using two kind of MF and their performance was evaluated.

**5.2 FUZZIFICATION**

In this step all crisp values were converted to linguistic values. Different linguistic term used for different input and output variables are given in table below.

**Table 5.1 Fuzzification of variables**

<b>Input and Output</b>	<b>Linguistic Variables</b>
Feed	low, high
Speed	low, medium, high
Drill diameter	low, medium, high
Point angle	low, medium, high
Surface roughness	lowest, lower, low, medium, high, higher, highest
Material removal rate	low, low-medium, medium, hi-medium, high

**5.3 MEMBERSHIP FUNCTIONS**

A membership function (MF) is a curve that defines how each point in the input space is mapped to a membership value (or degree of membership) between 0 and 1. In the present case two type of MF namely triangular and trapezoidal are considered.

### 5.3.1 TRIANGULAR MF

The simplest membership functions are formed using straight lines. So it is simplest membership function, and it has the function name ‘trimf’. This function is nothing more than a collection of three points forming a triangle. The triangular curve is a function of a vector,  $x$ , and depends on three scalar parameters  $a$ ,  $b$ , and  $c$ , as given by

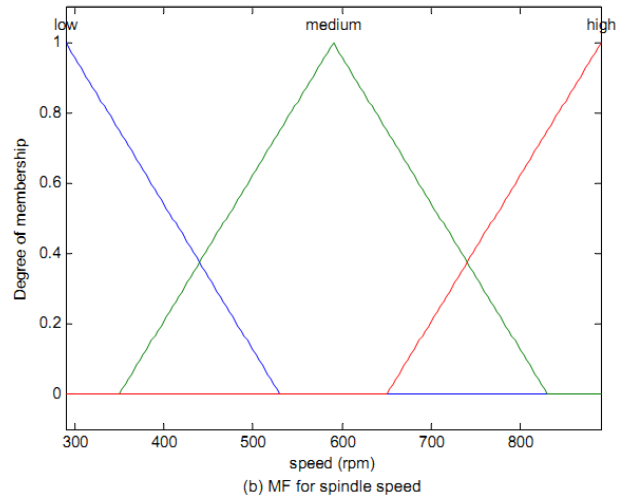
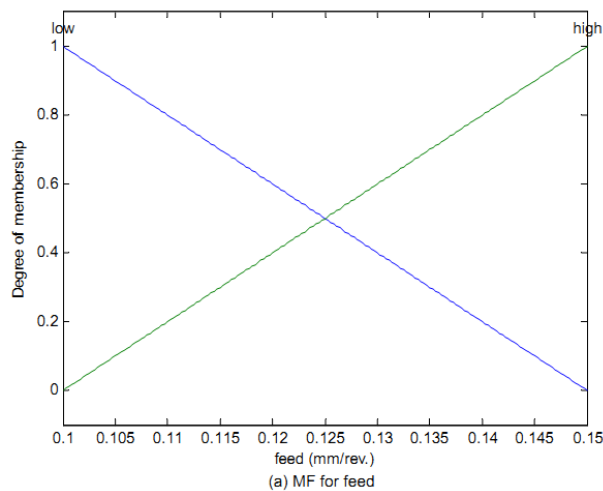
$$f(x,a,b,c) = \begin{cases} 0, & x \leq a \\ \frac{x-a}{b-a}, & a \leq x \leq b \\ \frac{c-x}{c-b}, & b \leq x \leq c \\ 0, & c \leq x \end{cases}$$

or, more compactly, by

$$f(x,a,b,c) = \max\left(\min\left(\frac{x-a}{b-a}, \frac{c-x}{c-b}\right), 0\right)$$

The parameters  $a$  and  $c$  locate the "feet" of the triangle and the parameter  $b$  locates the peak.

Different MF used for input and output are shown in figure below. Figure 5.1 a, b, c and d are representing different input MF for feed, speed, drill diameter and point angle. Figure e and f are representing output MF for SR and MRR respectively. Different MF of variables are taken as given in table 5.1 above. Abscissa of different variables is representing their range and ordinate is showing their degree of membership associated with drilling system.



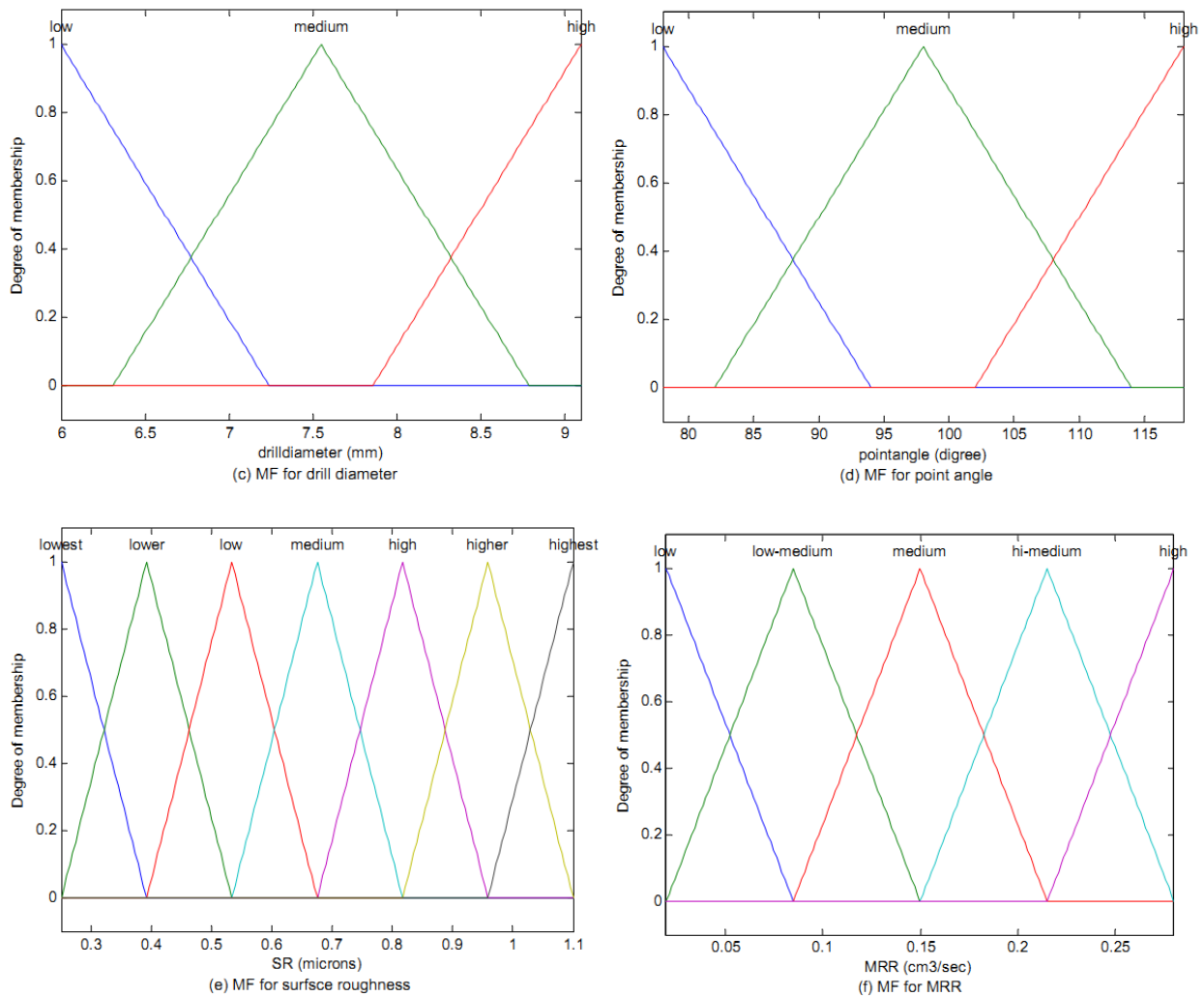


**Figure 5.1 Triangular MF for input and output parameters (a) MF for feed, (b) MF for spindle speed, (c) MF for drill diameter, (d) MF for point angle, (e) MF for SR, (f) MF for MRR**

### 5.3.2 TRAPEZOIDAL MF

It has a flat top and really is just a truncated triangle curve. it has the function name ‘trapmf’. The trapezoidal curve is a function of a vector,  $x$ , and depends on four scalar parameters  $a$ ,  $b$ ,  $c$ , and  $d$ , as given by

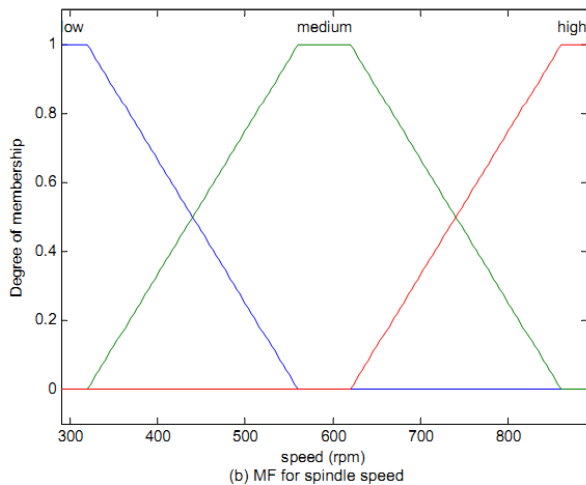
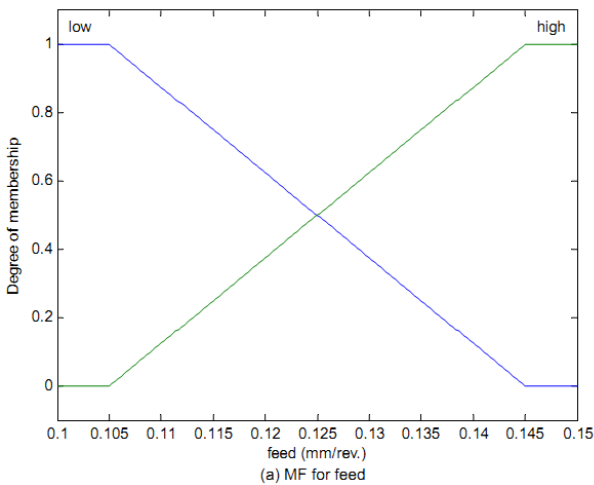
$$f(x; a, b, c, d) = \begin{cases} 0, & x \leq a \\ \frac{x-a}{b-a}, & a \leq x \leq b \\ 1, & b \leq x \leq c \\ \frac{d-x}{d-c}, & c \leq x \leq d \\ 0, & d \leq x \end{cases}$$

or, more compactly, by

$$f(x; a, b, c, d) = \max\left(\min\left(\frac{x-a}{b-a}, 1, \frac{d-x}{d-c}\right), 0\right)$$

The parameters a and d locate the "feet" of the trapezoid and the parameters b and c locate the "shoulders."

Different input and output MF used are shown below, Figure 5.2 a, b, c and d are representing different input MF for feed, speed, drill diameter and point angle. Figure e and f are representing output MF for SR and MRR respectively. Different MF of variables are taken as given in table 5.1 above. Abscissa of different variables is representing their range and ordinate is showing their degree of membership associated with drilling system. For feed only 2 MF (Low & High) were chosen and all remaining I/P variables have 3 MF (Low Medium High). For output variables 7 & 5 MF were selected for SR and MRR respectively to model the system.



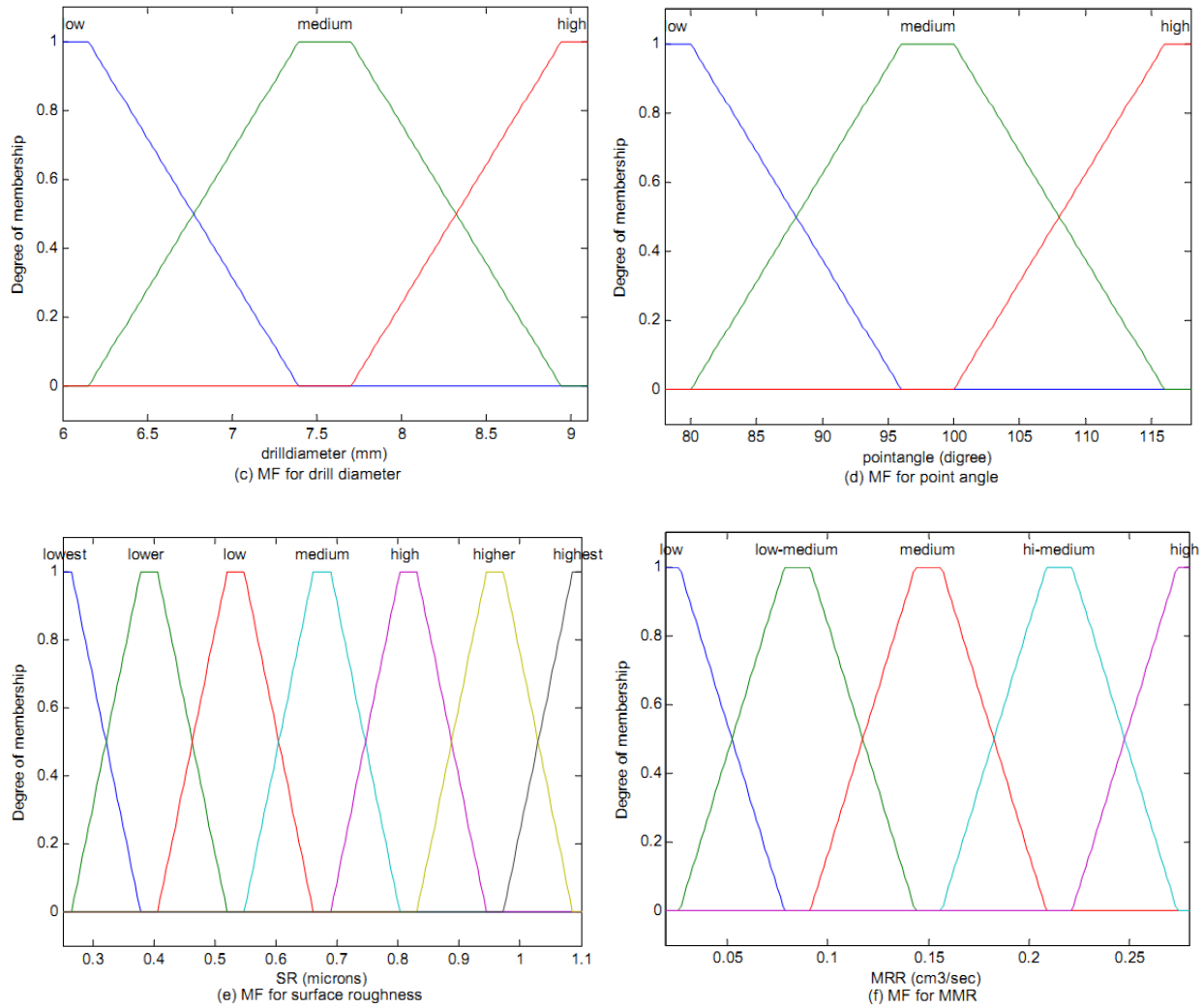


**Figure 5.2 Trapezoidal MF for input and output parameters (a) MF for feed, (b) MF for spindle speed, (c) MF for drill diameter, (d) MF for point angle, (e) MF for SR, (f) MF for MRR**

## 5.4 RULE EVALUATION

The fuzzy rule base consists of a group of IF-THEN statements. These IF-THEN rule statements are used to formulate the conditional statements that comprise fuzzy logic.

In this case 18 rule were developed based on the experimental conditions. In present case with four inputs,  $x_1, x_2, x_3, x_4$  and two outputs  $y_1$  and  $y_2$ , rules take the form,

Rule 1 : if  $x_1$  is  $A_1$  and  $x_2$  is  $B_1$  and  $x_3$  is  $C_1$  and  $x_4$  is  $D_1$  then  $y_1$  is  $E_1$  and  $y_2$  is  $F_1$ :else

Rule 2 : if  $x_1$  is  $A_2$  and  $x_2$  is  $B_2$  and  $x_3$  is  $C_2$  and  $x_4$  is  $D_2$  then  $y_1$  is  $E_2$  and  $y_2$  is  $F_2$ :else

Rule n : if  $x_1$  is  $A_n$  and  $x_2$  is  $B_n$  and  $x_3$  is  $C_n$  and  $x_4$  is  $D_n$  then  $y_1$  is  $E_n$  and  $y_2$  is  $F_n$

where  $A_i$ ,  $B_i$ ,  $C_i$ ,  $D_i$ ,  $E_i$  and  $F_i$  are linguistic values defined by fuzzy sets on the ranges (universes of discourse)  $X_i$  and  $Y_i$ , respectively. The if-part of the rule "x is A" is called the antecedent or premise, while the then-part of the rule "y is B" is called the consequent or conclusion.

IF-THEN rules for triangular MF are shown below

1. (feed==low) & (speed==low) & (drilldiameter==low) & (pointangle==low) => (SR=lowest)(MRR=low) (1)

2. (feed==low) & (speed==low) & (drilldiameter==medium) & (pointangle==medium) => (SR=lower)(MRR=low) (1)

3. (feed==low) & (speed==low) & (drilldiameter==high) & (pointangle==high) => (SR=lower)(MRR=low-medium) (1)

4. (feed==low) & (speed==medium) & (drilldiameter==low) & (pointangle==low) => (SR=lowest)(MRR=low) (1)

5. (feed==low) & (speed==medium) & (drilldiameter==medium) & (pointangle==medium) => (SR=low)(MRR=low-medium) (1)

6. (feed==low) & (speed==medium) & (drilldiameter==high) & (pointangle==high) => (SR=high)(MRR=medium) (1)

7. (feed==low) & (speed==high) & (drilldiameter==low) & (pointangle==medium) => (SR=lower)(MRR=low-medium) (1)

8. (feed==low) & (speed==high) & (drilldiameter==medium) & (pointangle==high) => (SR=lowest)(MRR=medium) (1)

9. (feed==low) & (speed==high) & (drilldiameter==high) & (pointangle==low) => (SR=lower)(MRR=hi-medium) (1)

10. (feed==high) & (speed==low) & (drilldiameter==low) & (pointangle==high) => (SR=low)(MRR=low) (1)

11. (feed==high) & (speed==low) & (drilldiameter==medium) & (pointangle==low) => (SR=medium)(MRR=low-medium) (1)

12. (feed==high) & (speed==low) & (drilldiameter==high) & (pointangle==medium) => (SR=highest)(MRR=low-medium) (1)

13. (feed==high) & (speed==medium) & (drilldiameter==low) & (pointangle==medium) => (SR=low)(MRR=low-medium) (1)

14. (feed==high) & (speed==medium) & (drilldiameter==medium) & (pointangle==high) => (SR=low)(MRR=low-medium) (1)

15. (feed==high) & (speed==medium) & (drilldiameter==high) & (pointangle==low) => (SR=high)(MRR=medium) (1)

16. (feed==high) & (speed==high) & (drilldiameter==low) & (pointangle==high) => (SR=low)(MRR=medium) (1)

17. (feed==high) & (speed==high) & (drilldiameter==medium) & (pointangle==low) => (SR=lower)(MRR=medium) (1)

18. (feed==high) & (speed==high) & (drilldiameter==high) & (pointangle==medium) => (SR=higher)(MRR=high) (1)

Similarly IF-THEN rules for trapezoidal MF were developed.

### 5.5 DEFUZZIFICATION

The input for the defuzzification process is a fuzzy set (the aggregate output fuzzy set) and the output is a single number. In the present case centroid defuzzification was selected which returns the center of area under the curve. Defuzzifier window for triangular MF function is shown below. For triangular MF the defuzzifier is shown below.

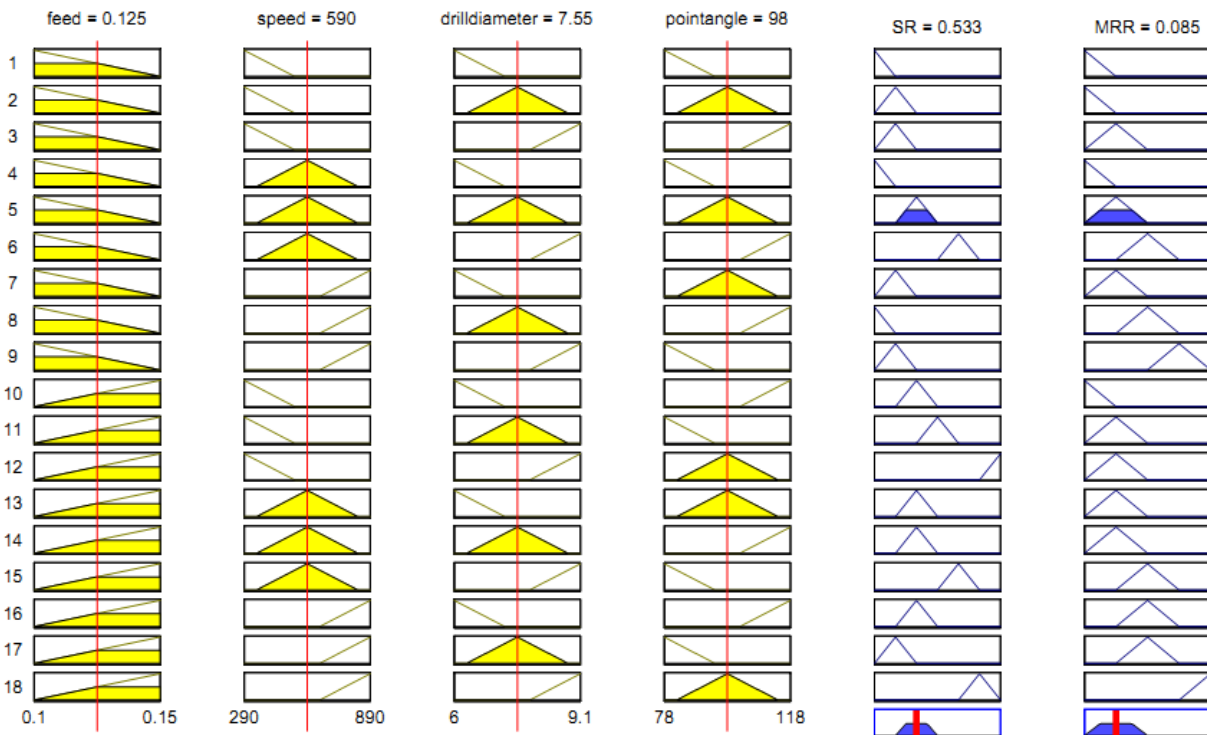
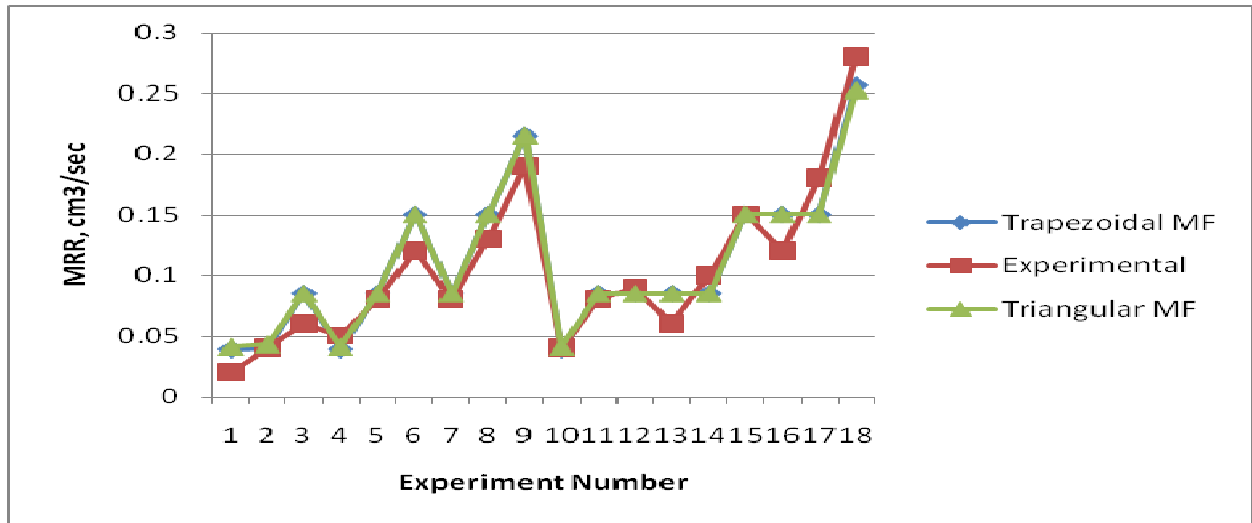


Figure 5.3 Defuzzifier for Triangular MF

## 5.6 ANALYSIS OF FUZZY RESULTS

The graph below is presenting the variation of MRR with experimental trial runs. The other two plots are of triangular and trapezoidal MF predicted values of MRR. From graph it is clear that there is very minute difference between experimental values and predicted values.



**Figure 5.4 Predicted Vs Experimental MRR**

The graph below is presenting the variation of SR with experimental trial runs. The other two plots are of triangular and trapezoidal MF predicted values of SR. From graph it is clear that there is very minute difference between experimental values and predicted values.

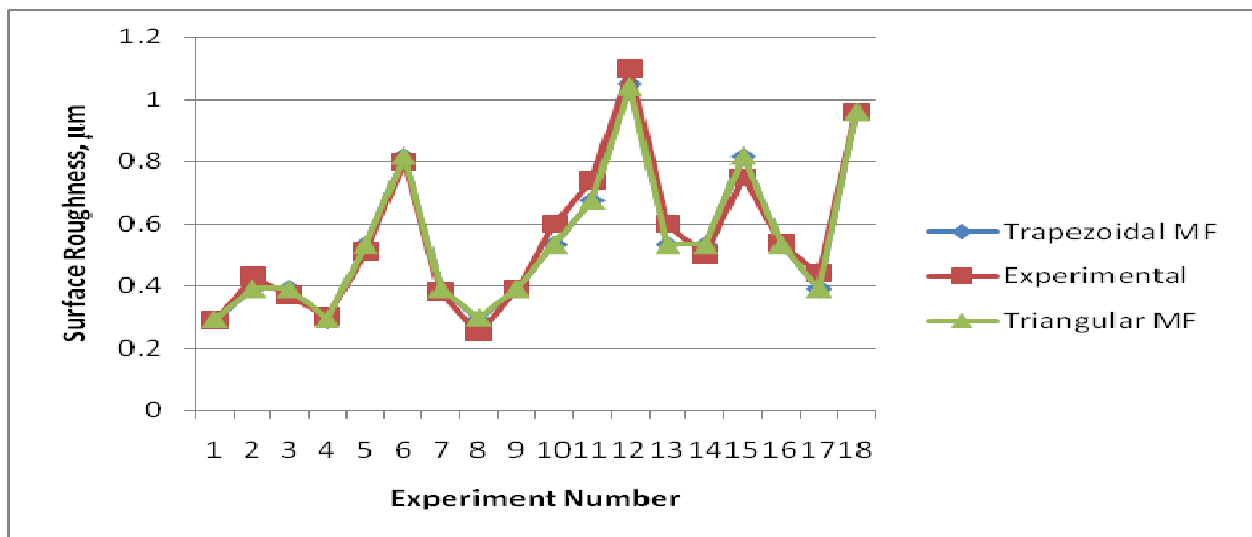


**Figure 5.5 Predicted Vs Experimental SR**

### 5.6.1 CORRELATION GRAPHS

The graph below (fig. 5.6 & 5.7) is representing the efficiency of triangular MF and trapezoidal MF in predicting the SR value for the drilling operation.  $R^2$  value is used for this purpose which is also known as 'coefficient of determination'. Its value ranges between 0 and 1. Higher the  $R^2$  value better is response.

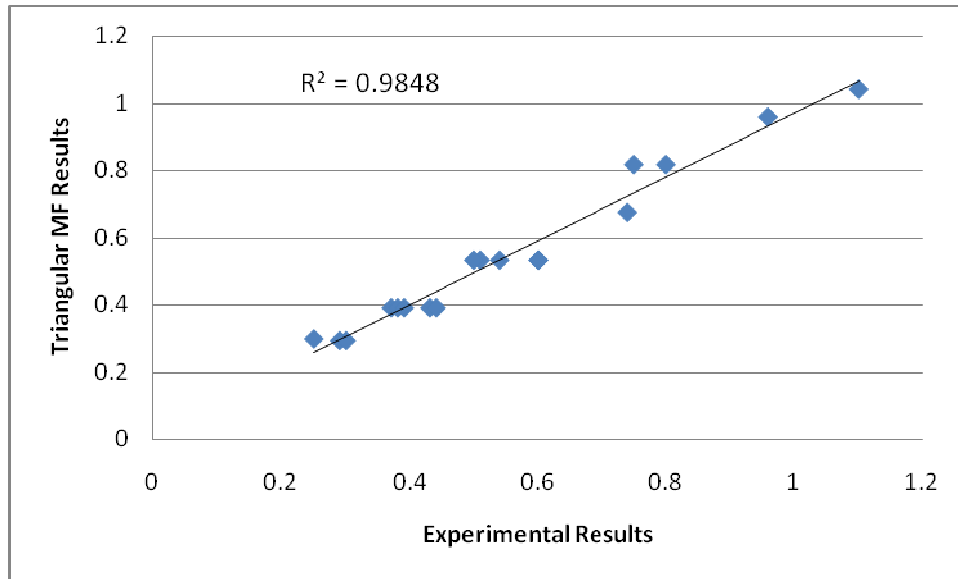


Figure 5.6 Correlation graph for triangular MF for SR

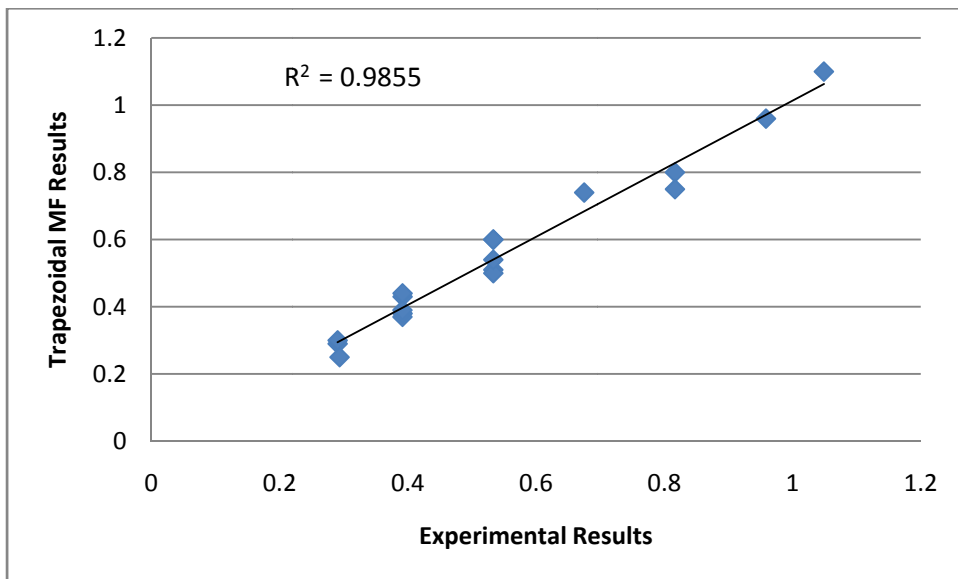
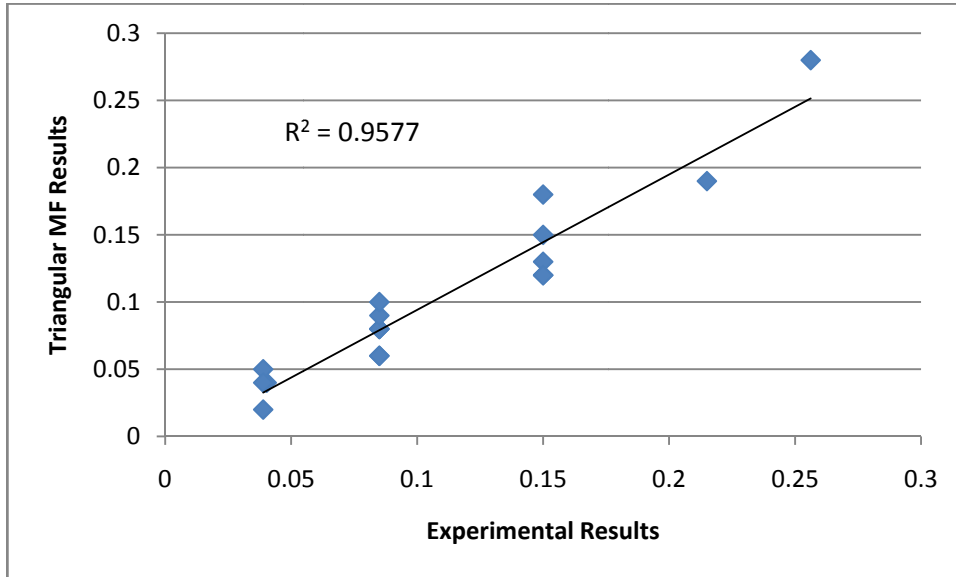
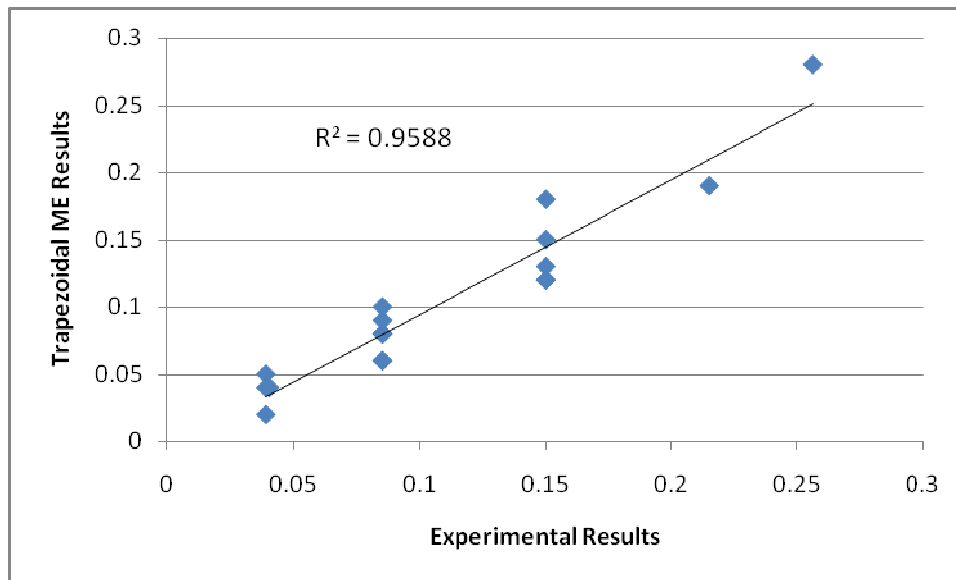


Figure 5.7 Correlation graph for trapezoidal MF for SR

From the above figures (5.7 & 5.8) we inferred that trapezoidal MF have larger efficiency which 98.55% than the triangular MF for predicting the SR. So for the present system trapezoidal MF should be used. The graph below (fig. 5.8 & 5.9) is representing the efficiency of triangular MF and trapezoidal MF in predicting the MRR value for the drilling operation. Here triangular MF showing 95.77% efficiency in predicting the MRR value and trapezoidal MF showing 95.88% efficiency. Again it was found that trapezoidal MF have larger efficiency.



**Figure 5.8 Correlation graph for triangular MF for MRR**



**Figure 5.9 Correlation graph for trapezoidal MF for MRR**

From above results it can be observed that trapezoidal MF are more efficient than triangular MF for the present system. As they are showing larger efficiency in predicting both MRR and SR, so they should be used for modeling the present drilling system.

### 5.6.2 RESPONSE SURFACE PLOTS

Response surface plot are plots between response characteristics on Z-axis and affecting parameters on the X & Y axis.

Figure 5.10 & 5.11 are representing the response surface plot between different parameters for SR. From figure 5.10 we get information that SR is good when choose high spindle speed which is above 800 rpm and lowest SR is observed at high value of point angle above from 100 degree. If we take spindle speed below 600 rpm and point angle below 80 degree then poor surface finish will be observed. Good finish is also observed if we take low point angle with high speed. Figure 5.11 is presenting response surface plot between drill diameter and point angle for SR. From the plot we conclude that low drill diameter is favorable for good finished surface. And again high point angle is responsible for good surface.

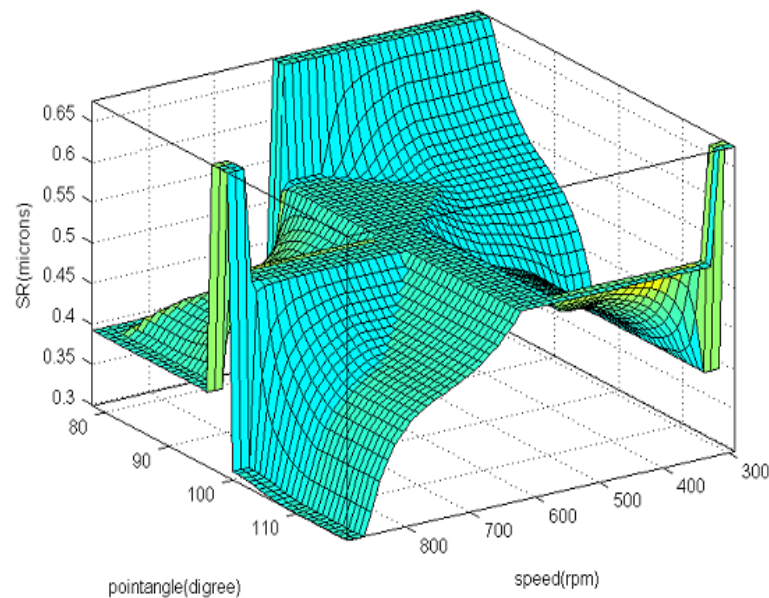


**Figure 5.10 Response surface between point angle and speed for SR**

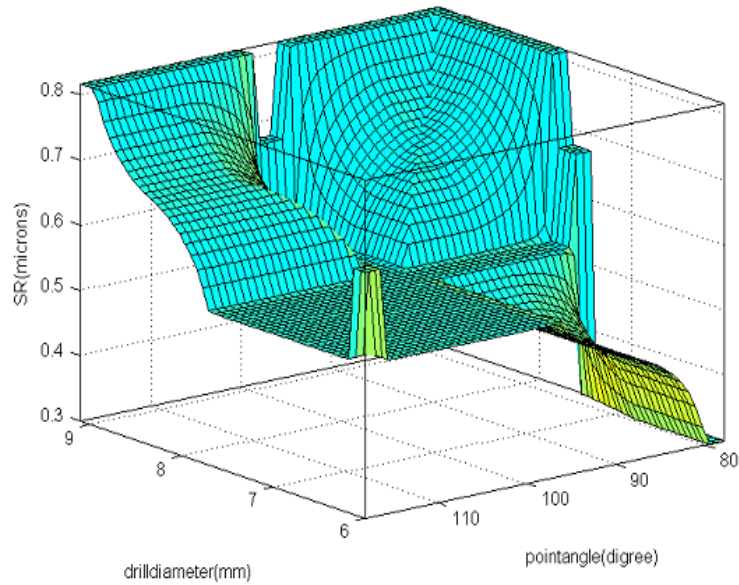


**Figure 5.11 Response surface between point angle and drill diameter for SR**

SR is increasing with the increase in drill diameter. Good finish is observed between drill diameter of 6-8 mm with a point angle range of 90-118 degree and finest finish is observed when we take point angle below 80 degree with drill diameter from 6 to 7.5 mm. Figure 5.12 & 5.13 are representing the response surface plot between different parameters for MRR. From figure 5.12 we get found that MRR is high when we take high spindle speed and there is less effect of point angle. Figure 5.13 is presenting response surface plot between drill diameter and point angle for MRR. From the plot we conclude that high drill diameter is favorable for high MRR. And again high point angle is less responsible for good MRR.

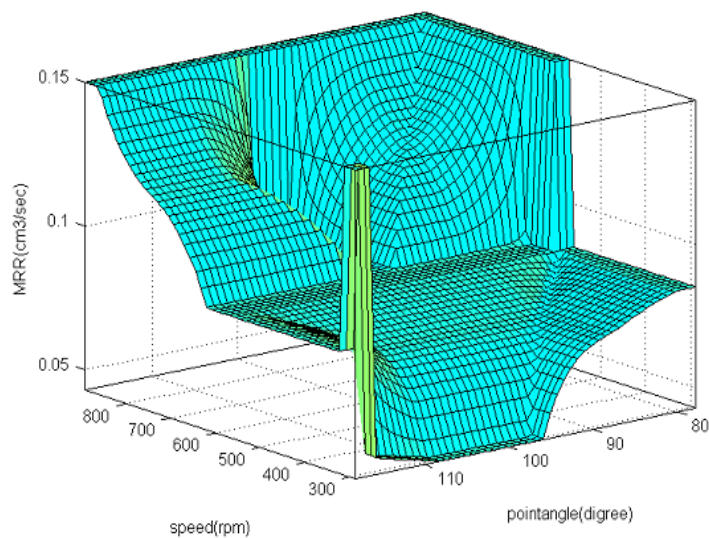


**Figure 5.12 Response surface between point angle and speed for MRR**

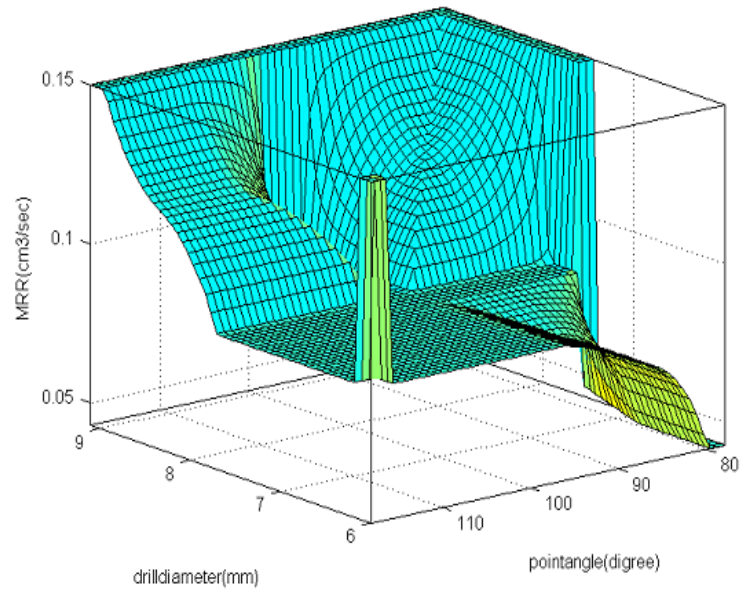


**Figure 5.13 Response surface between point angle and drill diameter for MRR**

From both the figure (5.12 & 5.13) it was found that only drill diameter and spindle speed are affecting the MRR and there is less influence of point angle.

From the different response surface plots for SR and MRR with different parameters it can be asserted that with the increase in drill diameter contact area between drill and w/p is get increased which increases the SR, on the other hand with the increase in spindle speed the material is removed at higher rate which increases the surface finish. While with the increase in spindle speed machining time is get reduced which inflate the MRR and also with the increase of drill diameter the volume of material removed is also get increased as the hole diameter is get increased, which subsequently increases the MRR.

#### 6.1 RESULTS AND DISCUSSION

The effect of parameters i.e. feed, speed, drill diameter and point angle and some of their interactions were evaluated using ANOVA and factorial design analysis. The purpose of the ANOVA was to identify the important parameters in prediction of MRR, TWR and SR. Some results consolidated from ANOVA and fuzzy modeling are given below,

##### 6.1.1 MRR

Factors affecting MRR were found to be feed, speed and drill diameter with their highest level. The contributions of feed, speed and drill diameter was 7.77%, 49.30% and 30.21% respectively. In S/N ratio study of MRR in addition to above factors interaction between feed and speed was also found significant. Their contribution was found feed (15.99%), speed (53.02%), drill diameter (34.39%) and interaction between feed and speed (1.40%). The mean value of MRR was found 8029.92 mm<sup>3</sup>/min with confidence interval of 0.028.

##### 6.1.2 SR

Factor affecting SR were found to be feed, drill diameter, point angle and interaction between interaction between feed & speed. The contribution of feed, drill diameter, point angle and of interaction between feed and speed was 35.67%, 27.16%, 9.55%, and 8.76% respectively. In S/N ratio study of SR except the interaction between feed and speed and speed all factors were significant and their contribution were found 41.51%, 20.61%, and 7.82% respectively. Their estimated mean was found 0.12 μm with confidence interval of 0.15.

##### 6.1.3 TWR

As no tool wear was observed during factorial design experimentation, but wear of tool was studied with 6 mm drill bit at 890 rpm with coarse feed (0.15 mm/rev.). The wear was found rapid at first stage after that wear was slow. Tool wear after 10 was found 22.148 mm and after that sudden increase in wear was observed which reached to 51.22 mm then small increment in wear of 4.33 mm was observed after 30 hole.

#### **6.1.4 FUZZY MODELING**

Fuzzy modeling of the drilling system was done and found that it can applied to this system as it predicted the MRR and SR with 95.88% and 98.55% efficiency respectively when trapezoidal MFs were used. In the modeling of system it was found that triangular MFs are less efficient as their efficiency to predict MRR and SR was found 95.77% and 98.48% respectively.

## REFERENCES

---

1. Youssef, H.A. & El-Hofy, H., (2008), “Machining Technology : Machine Tools and Operations”, CRC Press, ISBN - 978-1420043396.
2. Campbell, F.C., (2004), “Manufacturing Processes for Advanced Composites”, Elsevier Science, ISBN - 1856174158.
3. B. Latha and V. S. Senthilkumar (2010), Modeling and Analysis of Surface Roughness Parameters in Drilling GFRP Composites Using Fuzzy Logic, *Materials and Manufacturing Processes*, 25:8, 817-827.
4. ISO 1302 – 2001, Basic Components & Elements of Surface Topography.
5. J. Paulo Davim, (2010), *Machining Fundamentals and Recent Advances*”, Springer, ISBN - 978-1-84800-212-8.
6. Latha, B., &Senthilkumar, V.S. (2009).Analysis of Thrust Force in Drilling Glass Fiber-Reinforced Plastic Composites Using Fuzzy Logic, *Materials and Manufacturing Processes*, vol.24, 509-516.
7. Rajmohan, T., &Palanikumar, K. (2011).Experimental Investigation and Analysis of Thrust Force in Drilling Hybrid Metal Matrix Composites by Coated Carbide Drills, *Materials and Manufacturing Processes*, vol. 26, 961-968.
8. Patra, K., Pal, S.K., &Bhattacharyya, K. (2007).Application of wavelet packet analysis in drill wear monitoring, *Machining Science and Technology*, vol. 11, 413-432.
9. Gajate, A., Haber, R.E., Vega, P.I., &Alique, J.R. (2010).A Transductive Neuro-Fuzzy Controller: Application to a Drilling Process. *IEEE transactions on neural networks*, vol. 21, 1158-1167.
10. Krishnamoorthy, A., Sarathy, R.V., Boopathy, S.R., &Palanikumar, K. (2010).Modeling of Thrust Force in Drilling of CFRP Composites Using Adaptive Neuro Fuzzy Inference System. *IEEE*, 60-67.
11. Haber, R.E., Toro, R.M., & Gajate, A. (2010).Optimal fuzzy control system using the cross-entropy method. A case study of a drilling process. *Information Sciences*, vol. 180, 2777–2792.

12. Haber, R.E., Gajate, A., &Toro, R.M. (2009).Neurofuzzy Force-based Control in an Ethernet-based Application. A Case Study on a Drilling Process. *The 3<sup>rd</sup> international conference on innovation and computing information and control, IEEE*.
13. Iqbal, A., He, N., Dar, N. U., &Li, L. (2007).Comparison of fuzzy expert system based strategies of offline and online estimation of flank wear in hard milling process. *Expert Systems with Applications*, vol. 33, 61–66.
14. Panda, S.S., Chakraborty, D., &Pal, S.K. (2008).Flank wear prediction in drilling using back propagation neural network and radial basis function network. *Applied Soft Computing*, vol. 8, 858–871.
15. Metin Ertunc, H., Oysu, C. (2004), Drill wear monitoring using cutting force signals, *Mechatronics*, vol. 14, 533–548.
16. Velayudham, A., R. Krishnamurthy and T. Soundarapandian (2004), Evaluation of drilling characteristics of high volume fraction fibre glass reinforced polymeric composite, *International Journal of Machine Tools & Manufacture*, vol. 45, 399–406.
17. Uysal,A., & Altan,M. & Altan,E. (2012), Effects of cutting parameters on tool wear in drillingof polymer composite by Taguchi method, *Int J Adv Manuf Technol*, vol. 58, 915–921.
18. Iliescu,D., Gehin,D. , Gutierrez,M.E., F. Girota, F.(2010), Modeling and tool wear in drilling of CFRP, *International Journal of Machine Tools & Manufacture*, vol.50, 204–213.
19. Abu-Mahfouz, I (2003), Drilling wear detection and classification using vibration signals and artificial neural network, *International Journal of Machine Tools & Manufacture*, vol. 43, 707–720.
20. Panda, S.S., Singh, A.K., Chakraborty,D., Pal, S.K. (2006), Drill wear monitoring using back propagation neural network, *Journal of Materials Processing Technology*, vol.172, 283–290.
21. Kilickap, E., &Huseyinoglu, M. (2010).Selection of Optimum Drilling Parameters on Burr Height Using Response Surface Methodology and Genetic Algorithm in Drilling of AISI 304 Stainless Steel, *Materials and Manufacturing Processes*, vol. 25, 1068-1076.
22. Wang, J., Zhang, Q., &Mathew, P. (2011).Optimization of cutting conditions in drilling operations with plane rake faced twist drills, *Machining Science and Technology*, vol. 15, 91-109.
23. Latha, B., &Senthilkumar, V.S. (2010).Modeling and Analysis of Surface Roughness Parameters in Drilling GFRP Composites Using Fuzzy Logic. *Materials and Manufacturing Processes*, vol. 25, 817-827.

24. Nandi, A.K., & Davim, J.P. (2009). A study of drilling performances with minimum quantity of lubricant using fuzzy logic rules. *Mechatronics*, vol.19, 218–232.
25. K. Palanikumar (2010), Modeling and Analysis of Delamination Factor and Surface Roughness in Drilling GFRP Composites, *Materials and Manufacturing Processes*, vol.25, 1059-1067.
26. Tsao, C.C. (2005), The effect of pilot hole on delamination when core drill drilling composite materials, *International Journal of Machine Tools & Manufacture*, vol. 46, 1653–1661.
27. Tsao, C.C. and Hocheng, H. (2004), Effect of eccentricity of twist drill and candle stick drill on delamination in drilling composite materials, *International Journal of Machine Tools & Manufacture*, vol. 45, 125–130.
28. Faraz, A., Biermann, D., Weinert, K. (2009), Cutting edge rounding: An innovative tool wear criterion in drilling CFRP composite laminates, *International Journal of Machine Tools & Manufacture*, vol.49, 1185–1196.
29. Ross Phillip J., (1990), “Taguchi Techniques for Quality Engineering”, McGraw-Hill, ISBN 0-07-053866-2.

---

---

**MATLAB CODE FOR DRILLING PROCESS MODELING****TRIANGULAR MF**

```
[System]
Name='drilling'
Type='mamdani'
Version=2.0
NumInputs=4
NumOutputs=2
NumRules=18
AndMethod='min'
OrMethod='max'
ImpMethod='min'
AggMethod='max'
DefuzzMethod='centroid'

[Input1]
Name='feed'
Range=[0.1 0.15]
NumMFs=2
MF1='low':'trimf',[0.05 0.1 0.15]
MF2='high':'trimf',[0.1 0.15 0.2]

[Input2]
Name='speed'
Range=[290 890]
NumMFs=3
MF1='low':'trimf',[50 290 530]
MF2='medium':'trimf',[350 590 830]
MF3='high':'trimf',[650 890 1130]

[Input3]
Name='drilldiameter'
Range=[6 9.1]
NumMFs=3
MF1='low':'trimf',[4.76 6 7.24]
MF2='medium':'trimf',[6.31 7.55 8.79]
MF3='high':'trimf',[7.86 9.1 10.34]

[Input4]
Name='pointangle'
Range=[78 118]
NumMFs=3
MF1='low':'trimf',[62 78 94]
MF2='medium':'trimf',[82 98 114]
MF3='high':'trimf',[102 118 134]
```

```
[Output1]
Name='SR'
Range=[0.25 1.1]
NumMFs=7
MF1='lowest':'trimf',[0.1083 0.25 0.3917]
MF2='lower':'trimf',[0.25 0.3917 0.5333]
MF3='low':'trimf',[0.3917 0.5333 0.675]
MF4='medium':'trimf',[0.5333 0.675 0.8167]
MF5='high':'trimf',[0.675 0.8167 0.9583]
MF6='higher':'trimf',[0.8167 0.9583 1.1]
MF7='highest':'trimf',[0.9583 1.1 1.242]
```

```
[Output2]
Name='MRR'
Range=[0.02 0.28]
NumMFs=5
MF1='low':'trimf',[-0.045 0.02 0.085]
MF2='low-medium':'trimf',[0.02 0.085 0.15]
MF3='medium':'trimf',[0.085 0.15 0.215]
MF4='hi-medium':'trimf',[0.15 0.215 0.28]
MF5='high':'trimf',[0.215 0.28 0.345]
```

```
[Rules]
1 1 1 1, 1 1 (1) : 1
1 1 2 2, 2 1 (1) : 1
1 1 3 3, 2 2 (1) : 1
1 2 1 1, 1 1 (1) : 1
1 2 2 2, 3 2 (1) : 1
1 2 3 3, 5 3 (1) : 1
1 3 1 2, 2 2 (1) : 1
1 3 2 3, 1 3 (1) : 1
1 3 3 1, 2 4 (1) : 1
2 1 1 3, 3 1 (1) : 1
2 1 2 1, 4 2 (1) : 1
2 1 3 2, 7 2 (1) : 1
2 2 1 2, 3 2 (1) : 1
2 2 2 3, 3 2 (1) : 1
2 2 3 1, 5 3 (1) : 1
2 3 1 3, 3 3 (1) : 1
2 3 2 1, 2 3 (1) : 1
2 3 3 2, 6 5 (1) : 1
```

## **TRAPEZOIDAL MF**

```
[System]
Name='drillingt'
Type='mamdani'
Version=2.0
NumInputs=4
NumOutputs=2
```

```

NumRules=18
AndMethod='min'
OrMethod='max'
ImpMethod='min'
AggMethod='max'
DefuzzMethod='centroid'

[Input1]
Name='feed'
Range=[0.1 0.15]
NumMFs=2
MF1='low': 'trapmf',[0.055 0.095 0.105 0.145]
MF2='high': 'trapmf',[0.105 0.145 0.155 0.195]

[Input2]
Name='speed'
Range=[290 890]
NumMFs=3
MF1='low': 'trapmf',[20 260 320 560]
MF2='medium': 'trapmf',[320 560 620 860]
MF3='high': 'trapmf',[620 860 920 1160]

[Input3]
Name='drilldiameter'
Range=[6 9.1]
NumMFs=3
MF1='low': 'trapmf',[4.605 5.845 6.155 7.395]
MF2='medium': 'trapmf',[6.155 7.395 7.705 8.945]
MF3='high': 'trapmf',[7.705 8.945 9.255 10.49]

[Input4]
Name='pointangle'
Range=[78 118]
NumMFs=3
MF1='low': 'trapmf',[60 76 80 96]
MF2='medium': 'trapmf',[80 96 100 116]
MF3='high': 'trapmf',[100 116 120 136]

[Output1]
Name='SR'
Range=[0.25 1.1]
NumMFs=7
MF1='lowest': 'trapmf',[0.1225 0.2358 0.2642 0.3775]
MF2='lower': 'trapmf',[0.2642 0.3775 0.4058 0.5192]
MF3='low': 'trapmf',[0.4058 0.5192 0.5475 0.6608]
MF4='medium': 'trapmf',[0.5475 0.6608 0.6892 0.8025]
MF5='high': 'trapmf',[0.6892 0.8025 0.8308 0.9442]
MF6='higher': 'trapmf',[0.8308 0.9442 0.9725 1.086]
MF7='highest': 'trapmf',[0.9725 1.086 1.114 1.228]

[Output2]
Name='MRR'
Range=[0.02 0.28]
NumMFs=5
MF1='low': 'trapmf',[-0.0385 0.0135 0.0265 0.0785]
MF2='low-medium': 'trapmf',[0.0265 0.0785 0.0915 0.1435]

```

```
MF3='medium': 'trapmf', [0.0915 0.1435 0.1565 0.2085]
MF4='hi-medium': 'trapmf', [0.1565 0.2085 0.2215 0.2735]
MF5='high': 'trapmf', [0.2215 0.2735 0.2865 0.3385]
```

```
[Rules]
```

```
1 1 1 1, 1 1 (1) : 1
1 1 2 2, 2 1 (1) : 1
1 1 3 3, 2 2 (1) : 1
1 2 1 1, 1 1 (1) : 1
1 2 2 2, 3 2 (1) : 1
1 2 3 3, 5 3 (1) : 1
1 3 1 2, 2 2 (1) : 1
1 3 2 3, 1 3 (1) : 1
1 3 3 1, 2 4 (1) : 1
2 1 1 3, 3 1 (1) : 1
2 1 2 1, 4 2 (1) : 1
2 1 3 2, 7 2 (1) : 1
2 2 1 2, 3 2 (1) : 1
2 2 2 3, 3 2 (1) : 1
2 2 3 1, 5 3 (1) : 1
2 3 1 3, 3 3 (1) : 1
2 3 2 1, 2 3 (1) : 1
2 3 3 2, 6 5 (1) : 1
```